

Climate Dynamics

A first-of-its-kind multi-model convection permitting ensemble for investigating convective phenomena over Europe and the Mediterranean --Manuscript Draft--

Manuscript Number:	CLDY-D-17-00886R1
Full Title:	A first-of-its-kind multi-model convection permitting ensemble for investigating convective phenomena over Europe and the Mediterranean
Article Type:	S.I. : Advances in Convection-Permitting Climate Modeling
Keywords:	Convection-permitting; ensemble models; climate applications
Corresponding Author:	Erika Coppola Abdus Salam Centro internazionale di fisica teorica ITALY
Corresponding Author Secondary Information:	
Corresponding Author's Institution:	Abdus Salam Centro internazionale di fisica teorica
Corresponding Author's Secondary Institution:	
First Author:	Erika Coppola
First Author Secondary Information:	
Order of Authors:	Erika Coppola
	Stefan Sobolowski
	Emanuela Pichelli
	Francesca Raffaele
	Bodo Ahrens
	Ivonne Anders
	Nikolina Ban
	Sophie Bastin
	Michal Belda
	Danijel Belusic
	Alberto Caldas-Alvarez
	Rita Margarida Cardoso
	Silvio Davolio
	Andreas Dobler
	Jesus Fernandez
	Lluís Fita
	Quentin Fumiere
	Filippo Giorgi
	Klaus Goergen
	Ivan Guettler
	Tomas Halenka
	Dominikus Heinzeller

	Øivind Hodnebrog
	Daniela Jacob
	Stergios Kartsios
	Eleni Katragkou
	Elizabeth Kendon
	Samiro Khodayar
	Harald Kunstmann
	Sebastian Knist
	Álvaro Lavín
	Petter Lind
	Torge Lorenz
	Douglas Maraun
	Louis Marelle
	Erik van Meijgaard
	Josipa Milovac
	Gunnar Myhre
	Hans-Juergen Panitz
	Marie Piazza
	Mario Raffa
	Thomas Raub
	Burkhardt Rockel
	Christoph Schär
	Kevin Sieck
	Pedro M. M. Soares
	Samuel Somot
	Lidija Srnec
	Paolo Stocchi
	Merja Tölle
	Heimo Truhetz
	Robert Vautard
	Hylke de Vries
	Kirsten Warrach-Sagi
Order of Authors Secondary Information:	
Funding Information:	
Abstract:	A recently launched project under the auspices of the World Climate Research Program's (WCRP) Coordinated Regional Downscaling Experiments Flagship Pilot Studies program (CORDEX-FPS) is presented. This initiative aims to build first-of-its-kind ensemble climate experiments of convection permitting models to investigate present and future convective processes and related extremes over Europe and the Mediterranean. In this manuscript the rationale, scientific aims and approaches are presented along with some preliminary results from the testing phase of the project. Three test cases were selected in order to obtain a first look at the ensemble performance. The test cases covered a summertime extreme precipitation event over

Austria, a fall Foehn event over the Swiss Alps and an intensively documented fall event along the Mediterranean coast. The test cases were run in both "weather-like" (WL, initialized just before the event in question) and "climate" (CM, initialized one month before the event) modes. A total of 22 ensemble members, representing six different modeling systems with different physics and modelling chain options, was generated for the test cases (26 modeling teams have committed to perform the longer climate simulations). Results indicate that, when run in WL mode, the ensemble captures all three events quite well. They suggest that the more the event is driven by large-scale conditions, the closer the agreement between the ensemble members. Even in climate mode the large-scale driven events over the Swiss Alps and the Mediterranean coasts are still captured, but the inter-model spread increases as expected. In the case over Mediterranean the effects of local-scale interactions between flow and orography and land-ocean contrasts are readily apparent. However, there is a much larger, though not surprising, increase in the spread for the Austrian event, which was weakly forced by the large-scale flow. The preliminary results illustrate both the promise and the challenges that convection permitting modeling faces and make a strong argument for an ensemble-based approach to investigating high impact convective processes.

[Click here to view linked References](#)

1 **A first-of-its-kind multi-model convection permitting** 2 **ensemble for investigating convective phenomena over** 3 **Europe and the Mediterranean (submitted)**

4 E. Coppola¹, S. Sobolowski², E. Pichelli¹, F. Raffaele¹, B. Ahrens³, I. Anders⁴, N. Ban⁵, S.
5 Bastin⁶, M. Belda⁷, D. Belusic⁸, A. Caldas-Alvarez⁹, R. M. Cardoso¹⁰, S. Davolio¹¹, A.
6 Dobler¹², J. Fernandez¹³, L. Fita¹⁴, Q. Fumiere¹⁵, F. Giorgi¹, K. Goergen^{16,17}, I. Güttler¹⁸, T.
7 Halenka⁷, D. Heinzeller^{19,20}, Ø. Hodnebrog²¹, D. Jacob²², S. Kartsios²³, E. Katragkou²³, E.
8 Kendon²⁴, S. Khodayar⁹, H. Kunstmann^{19,25}, S. Knist^{26,17}, A. Lavín-Gullón²⁷, P. Lind⁸, T.
9 Lorenz², D. Maraun²⁸, L. Marelle²¹, E. van Meijgaard²⁹, J. Milovac³⁰, G. Myhre²¹, H.-J.
10 Panitz⁹, M. Piazza²⁸, M. Raffà³¹, T. Raub²², B. Rockel³², C. Schär⁵, K. Sieck²², P. M. M.
11 Soares¹⁰, S. Somot¹⁵, L. Srnec¹⁸, P. Stocchi¹¹, M. H. Tölle³³, H. Truhetz²⁸, R. Vautard⁶, H. de
12 Vries²⁹, K. Warrach-Sagi³⁰

13

- 14 1. International Centre for Theoretical Physics (International Center for Theoretical Physics
15 (ICTP)), Trieste, Italy
- 16 2. Uni Research, the Bjerknes Centre for Climate Research, Bergen, Norway.
- 17 3. Goethe-Universität Frankfurt a.M. Frankfurt/Main, Germany
- 18 4. ZAMG (Central Institute for Meteorology and Geodynamics), Vienna, Austria
- 19 5. Institute for Atmospheric and Climate Science, ETH Zürich, Zürich Switzerland
- 20 6. Institut Pierre Simon Laplace (IPSL), LATMOS, UVSQ, UPMC, CNRS, Guyancourt,
21 France
- 22 7. Charles University, Department of Atmospheric Physics, Faculty of Mathematics and
23 Physics, Prague, Czech Republic
- 24 8. Swedish Meteorological and Hydrological Institute (SMHI), Norrköping, Sweden
- 25 9. Karlsruhe Institute of Technology, Institute of Meteorology and Climate Research -
26 Troposphere Research, Karlsruhe, Germany
- 27 10. Instituto Dom Luiz, Faculdade de Ciências, Universidade de Lisboa
- 28 11. Institute of Atmospheric Sciences and Climate, National Research Council of Italy, CNR-
29 ISAC, Bologna, Italy
- 30 12. The Norwegian Meteorological institute, Oslo, Norway
- 31 13. Meteorology Group. Dept. Applied Mathematics and Computer Science. Universidad de
32 Cantabria, Santander, Spain
- 33 14. Centro de Investigaciones del Mar y la Atmósfera (CIMA), CONICET-UBA, CNRS
34 UMI-IFAECI, Buenos Aires, Argentina
- 35 15. CNRM (Centre National de Recherches Météorologiques), Université de Toulouse,
36 Météo-France, CNRS, Toulouse, France
- 37 16. Institute of Bio- and Geosciences (Agrosphere, IBG-3), Research Centre Jülich, Jülich,
38 Germany
- 39 17. Centre for High-Performance Scientific Computing in Terrestrial Systems, Geoverbund
40 ABC/J, Jülich, Germany
- 41 18. Meteorological and Hydrological Service (DHMZ), Zagreb, Croatia

- 42 19. Institute of Meteorology and Climate Research (IMK-IFU), Karlsruhe Institute of
43 Technology (KIT), Kreuzeckbahnstr.19, 82467, Garmisch-Partenkirchen, Germany
44 20. National Oceanic and Atmospheric Administration, Earth System Research Laboratory,
45 Boulder, CO, USA
46 21. Center for International Climate and Environmental Research – Oslo (CICERO), Oslo,
47 Norway
48 22. Climate Service Center (CSC)Helmholtz-Zentrum Geesthacht Hamburg, Germany
49 23. Department of Meteorology and Climatology, School of Geology, Aristotle University of
50 Thessaloniki, Greece
51 24. Met Office Hadley Centre, Exeter, United Kingdom
52 25. Augsburg University, Institute of Geography, Augsburg, Germany
53 26. Meteorological Institute, University of Bonn, Bonn, Germany
54 27. Meteorology Group. Instituto de Física de Cantabria (IFCA). CSIC-Univ. Cantabria,
55 Santander, Spain
56 28. Wegener Center for Climate and Global Change (WEGC), University of Graz,
57 Brandhofgasse 5, A-8010 Graz, Austria
58 29. Royal Netherlands Meteorological Institute (KNMI), de Bilt, Netherlands
59 30. Institute of Physics and Meteorology (IPM), University of Hohenheim, Stuttgart,
60 Germany
61 31. Euro-Mediterranean Center on Climate Change (CMCC Foundation)
62 32. Helmholtz-Zentrum Geesthacht
63 33. Department of Geography, Climatology, Climate Dynamics and Climate Change, Justus-
64 Liebig-University Giessen, Senckenbergstr. 1, 35390 Giessen, Germany

65
66
67
68
69
70
71
72
73
74
75

76 corresponding authors: Erika Coppola (coppolae@ictp.it), Stefan Sobolowski
77 (stefan.sobolowski@uni.no)

78
79

80 **Abstract**

81 A recently launched project under the auspices of the World Climate Research Program's
82 (WCRP) Coordinated Regional Downscaling Experiments Flagship Pilot Studies program

83 (CORDEX-FPS) is presented. This initiative aims to build first-of-its-kind ensemble climate
84 experiments of convection permitting models to investigate present and future convective
85 processes and related extremes over Europe and the Mediterranean. In this manuscript the
86 rationale, scientific aims and approaches are presented along with some preliminary results
87 from the testing phase of the project. Three test cases were selected in order to obtain a first
88 look at the ensemble performance. The test cases covered a summertime extreme
89 precipitation event over Austria, a fall Foehn event over the Swiss Alps and an intensively
90 documented fall event along the Mediterranean coast. The test cases were run in both
91 “weather-like” (WL, initialized just before the event in question) and “climate” (CM,
92 initialized one month before the event) modes. Ensembles of 18-21 members, representing
93 six different modeling systems with different physics and modelling chain options, was
94 generated for the test cases (27 modeling teams have committed to perform the longer climate
95 simulations). Results indicate that, when run in WL mode, the ensemble captures all three
96 events quite well with ensemble correlation skill scores of 0.67, 0.82 and 0.91. They suggest
97 that the more the event is driven by large-scale conditions, the closer the agreement between
98 the ensemble members. Even in climate mode the large-scale driven events over the Swiss
99 Alps and the Mediterranean coasts are still captured (ensemble correlation skill scores of 0.90
100 and 0.62, respectively), but the inter-model spread increases as expected . In the case over
101 Mediterranean the effects of local-scale interactions between flow and orography and land-
102 ocean contrasts are readily apparent. However, there is a much larger, though not surprising,
103 increase in the spread for the Austrian event, which was weakly forced by the large-scale
104 flow. Though the ensemble correlation skill score is still quite high (0.80). The preliminary
105 results illustrate both the promise and the challenges that convection permitting modeling
106 faces and make a strong argument for an ensemble-based approach to investigating high
107 impact convective processes.

108

109 **Introduction**

110

111 Recent years have witnessed an explosive increase in climate simulations being run at
112 convection permitting scales (so-called convection permitting regional climate modelling
113 (CP-RCM)). The types of models used in these experiments are generally, though not
114 exclusively, limited area models with grid spacings under 4 km (Prein et al. 2015).
115 Convection, and its related impacts, is of high interest to atmospheric scientists, climate
116 impacts researchers and the public due to the role it plays in driving damaging extreme events
117 such as heavy precipitation, floods, landslides, windstorms (Carvalho et al., 2002; Jakob and
118 Weatherly, 2003; Beniston, 2006; Ducrocq et al., 2014; Stucki et al., 2015). It is also the
119 dominant type of precipitation in many parts of the world, such as the tropics, and influences
120 the general circulation of the atmosphere through tropospheric mixing and cloud - circulation
121 interactions (e.g., Bony et al. 2015). Unfortunately, parameterization of convection, which is
122 required at the grid spacing of most Global Climate Models (GCMs) and Regional Climate
123 Models (RCMs), contributes to errors in climate simulations (Dirmeyer et al., 2012; Klein et
124 al., 2013). Poor representation of convection and related processes also likely contributes to
125 the uncertain response of the atmospheric circulation to changing greenhouse gas
126 concentrations (Shepherd, 2014; Sherwood et al., 2014; Webb et al., 2015). In addition to
127 errors related to convection, along with clouds and circulations associated with it, many other
128 physical parameterization schemes interact with models' convection schemes, raising the
129 potential for consequences in other aspects of a climate simulation (Stevens and Bony, 2013).
130 These twin desires, the reduction of model errors associated with parameterized convection
131 and a more detailed representation of present and future regional climate, have strongly
132 motivated the recent increase in modeling activities at convection permitting scales.

133

134 There is a rich history in the Numerical Weather Prediction (NWP) and mesoscale
135 meteorology communities of using convection permitting simulations for process and case
136 studies (e.g., Benoit et al., 2002; Milovac et al., 2016; Schwitalla et al., 2017). These
137 researchers have decades of experience running simulations at these resolutions and have
138 shown the added value of resolving convective scale phenomena such as complex
139 interactions with orography (e.g., Grell et al., 2000; Pontoppidan et al., 2017), precipitation
140 intensity (e.g., Ducrocq et al. 2002, 2008; Davis et al., 2006) and severe weather (e.g.,
141 Weisman, et al., 1997; Mass et al., 2002; Done et al., 2004; Khodayar et al., 2016). Although,
142 it should be noted that some authors advocate for a severe change of data assimilation
143 approaches, physics (e.g., microphysics), parameterizations and numerical methods to be
144 used at convection resolving scales (Yano et al., 2015; Yano et al., 2017). Until recently there
145 has not been as much attention to longer and scenario-based experiments (Kendon et al.
146 2012; Fosser et al. 2014; Prein et al. 2015). Further, climate change detection and attribution
147 studies at convection permitting scales have only just begun. This has been due mainly to
148 computational limitations and costs. With recent advances in processing speed and efficiency,
149 research teams with an eye towards improving our understanding of processes driving
150 societally relevant climate impacts, have begun developing and running CP-RCMs at climate
151 time scales.

152

153 A number of decade-long simulations have been completed in recent years with impressive
154 results (Kendon et al., 2012; Warrach-Sagi et al., 2013; Fosser et al. 2014; Ban et al., 2014;
155 Brisson et al., 2016; Déqué et al. 2016; Tölle et al. 2017). The benefits of running climate
156 simulations (~10 years or more) at convection permitting grid spacings are far reaching.
157 Among the improvements, compared to coarser resolution simulations, are a more accurate

158 representation of diurnal cycles, hourly precipitation intensities, local-regional circulations,
159 seasonal average precipitation, convective downdrafts, and the representation of cold pools
160 (Prein et al., 2013a, Ban et al., 2014; Fosser et al., 2014; Kendon et al., 2012, 2014;
161 Rasmussen et al., 2014; Brisson et al., 2016; Déqué et al. 2016; Fumière et al., this issue). In
162 addition to the direct effects of resolving convective processes, - there are additional benefits
163 through e.g., more accurate representation of interactions with complex topography, urban
164 effects, land-ocean contrasts and land surface heterogeneities, which play a key role in
165 forcing or triggering convection (Prein et al., 2013b). Convection-permitting climate
166 simulations also allow the study of complex and fine scale aerosol-cloud-precipitation
167 interactions as shown in Heinzeller et al. (2016). Finally, there are indications that CP-RCM
168 simulations have positive indirect effects on the representation of regional climate through
169 various feedback mechanisms such as soil moisture - precipitation (Hohenegger et al., 2009)
170 and soil moisture/vegetation - temperature (Tölle et al. 2014) and urban effects (Argüeso et
171 al., 2014). For example, there is indication for reduced mid-Europe summer warming (in its
172 mean and extremes) in CP-RCM simulations (Tölle et al. 2017). There is also evidence that
173 explicitly representing deep convection qualitatively modifies the response of summertime
174 convective extremes to climatic changes (Kendon et al., 2014; Meredith et al., 2015; Giorgi et
175 al. 2016; Tölle et al. 2017). For a comprehensive review see Prein et al. (2015).

176

177 However, there are limitations to CP-RCM. At these scales, shallow convection is not
178 explicitly resolved (e.g. Soares et al. 2004; Khairoutdinov and Randall 2006; Siebesma et al.,
179 2007) and is crucial in providing moisture and energy from the planetary boundary layer to
180 the free atmosphere, which sustains the development of deep convection (e.g. Holloway and
181 Neelin 2009). On one hand, summertime convective systems over land are strongly
182 determined by the transition from shallow to deep convection (Teixeira et al., 2008; Wu et

183 al., 2009), and on the other hand, shallow convection is directly linked to tropical deep
184 convection and other atmospheric phenomena like the Madden-Julian oscillation (Teixeira et
185 al., 2011; Chen et al., 2016). Consequently, CP-RCM results are highly model-dependent.
186 This poses problems not only for developing a stronger process-based understanding of the
187 present climate but also for assessing robustness in future change signals. Also, single model
188 experiments are not particularly robust and do not sample the range of natural variability
189 (e.g., Tebaldi and Knutti, 2007; Deser et al., 2012). Up to now assessments of uncertainties in
190 future projections at km-scales have not been possible due to the prevalence of single model,
191 single realization experiments. This issue related to internal variability is moreover
192 exacerbated at finer spatial scales where local interactions play a more prominent role
193 (Hawkins and Sutton, 2009; Deser et al., 2014). Therefore, ensemble based approaches will
194 be needed in order to investigate convective extremes and related uncertainties in a climate
195 change context. Further to this point, "coordinated modeling programs are crucially needed to
196 advance parameterizations of unresolved physics and to assess the full potential of CPMs"
197 (Prein et al., 2015).

198

199 The confluence of activities around CP-RCM at climate scales, recent field campaigns
200 covering heavy precipitation and associated extreme events, and computational
201 advancements, suggest that the time is right for coordinated multi-model ensemble CP-RCM
202 experiments. In early 2016 a consortium of modeling groups from the Med-CORDEX and
203 Euro-CORDEX initiatives submitted an application for a targeted Flagship Pilot Study (FPS,
204 Gutowski et al. 2016) to the WCRP CORDEX (Coordinated Regional Downscaling
205 Experiment, Giorgi et al. 2009) program ([http://cordex.org/experiment-guidelines/flagship-
206 pilot-studies/](http://cordex.org/experiment-guidelines/flagship-pilot-studies/)). The aim is to develop a set of first-of-their-kind, multi-model ensemble
207 experiments at CP-RCM scales over Euro-Mediterranean region.

208

209 However, the project is much more than a set of multi-model ensemble experiments. We aim
210 to answer questions related to drivers of convective extremes across scales, event attribution
211 under changing climate conditions and more (see Scientific Aims below). For example, even
212 at convection permitting scales turbulence and other fine scale processes are not resolved and
213 model errors will still exist. Also, computational costs limit the length of simulations which
214 limits their utility in assessing uncertainty and trends. In this case, combined dynamical-
215 statistical approaches and process-informed bias correction may be of use (see, Maraun et al.,
216 2017). As mentioned previously, event detection and attribution is also just beginning and
217 this task likely requires a more nuanced approach to interpreting projections. One promising
218 avenue that the project will pursue is the construction of so-called “storylines” (e.g., Meredith
219 et al., 2015; Shepherd et al., 2014). Storylines’ may be thought of as an alternative way to
220 interpret large multi-model ensembles, where regional impacts are assessed over, for
221 example, a range plausible scenarios of atmospheric circulation change (as and example see,
222 Zappa and Shepherd, 2018).

223

224 The FPS was awarded in spring 2016. The first annual meeting was held in November of
225 2016 at the Abdus Salam International Centre for Theoretical Physics in Trieste, Italy. Work
226 began on finalizing scientific aims, developing an experimental protocol and selecting
227 representative test cases to be examined prior to launching into expensive decade-long
228 simulations. The primary objectives of the present manuscript are to 1) introduce the project,
229 2) describe its scientific goals and approaches and 3) show some preliminary results, which
230 illustrate both the promise and peril of CP-RCM in a multi-model ensemble context.

231

232 The next section provides background information on the FPS (motivation, aims, timeline),
233 followed by sections detailing methods and presenting preliminary results. The paper finishes
234 with a discussion of the way forward and an invitation for contributions to the broader CP-
235 RCM community.

236 **FPS description**

237 *Motivation*

238

239 Much of the motivation for the project is provided in the previous section. In short: Climate
240 change can alter the character of convection, making extreme precipitation more extreme, and
241 also potentially modify large-scale conditions (atmospheric circulation and stratification) that
242 favor convection. This can then induce changes in, e.g., return periods of precipitation
243 extremes, spatial and temporal distribution of events, the effects of convection-induced
244 feedback processes.

245

246 The study of convective events and their evolution under human-induced climate change is
247 therefore of particular importance, and it is also timely not least due to the following:

248

- 249 • Large field campaigns dedicated to the study of heavy precipitation events such
250 as HyMeX (Ducrocq et al., 2014), and gridded high-resolution precipitation
251 datasets (typically hourly, kilometer scale), often merging station and radar data
252 (Wüest et al. 2010, Tabary et al. 2012, Delrieu et al. 2014) now provide a wealth
253 of observations;
- 254 • Computer capacity and model development now allow limited-area convection-
255 permitting climate simulations at longer time-scales (Kendon et al., 2012, 2014;
256 Ban et al., 2014, 2015), enabling a leap in climate modeling capacity;

- 257 • Homogeneous observation data sets collected over the years can unveil emerging
258 trend signals in most extreme precipitation events, particularly at sub-daily time
259 scales (Westra et al., 2014), in Mediterranean coastal areas (Vautard et al. 2015)
260 and in Alpine mountain ranges (Scherrer et al. 2016)
- 261 • Several issues linked to detection, attribution and downscaling of the very
262 localized consequences of extreme convective events can now benefit from recent
263 progress in advanced statistical methods combined with advances in dynamical
264 modeling (Beaulant et al., 2011).

265

266 Convective extreme events are also a priority under the WCRP Grand Challenge on [weather](#)
267 [and climate extremes](#), because they carry both society-relevant and scientific challenges that
268 can be tackled in the coming years.

269

270 The proposed work in the Convection FPS also reflects a number of criteria identified by the
271 CORDEX-FPS Scientific Advisory Team (SAT) such as: i) run RCMs at a broad range of
272 resolutions, down to convection-permitting; ii) promote side-by-side experimental design and
273 evaluations of both statistical and dynamical downscaling techniques at scales more typical of
274 vulnerability-impacts-assessment applications; iii) Design targeted experiments aimed at
275 investigating specific regional processes and circulations; iv) investigate the importance of
276 regional scale forcings; v) Compile and use high quality, high resolution (both spatial and
277 temporal), multi-variable observation datasets for model validation and analysis of processes.

278

279 The makeup of the consortium is diverse, both institutionally and with respect to expertise
280 (Table 1). Though many participants come from climate background, others bring significant
281 NWP experience to the challenge. The FPS mobilizes the Euro-CORDEX and Med-

282 CORDEX communities but is also open to new partners who bring fresh perspectives and
283 expertise.

284

285 *Scientific questions*

286

287 The project was conceived with three general and open-ended scientific questions to allow
288 some flexibility in the analyses while also providing sufficient structure to keep the
289 consortium working towards some common goals. The general aims and specific
290 challenges/questions can be summarized as:

291

292 **1. How do convective events and associated damaging phenomena (heavy**
293 **precipitation, wind storms, flash-floods) respond to changing climate conditions in**
294 **different climatic regions of Europe?**

295

- 296 ● Identify trends in intensity, scale and duration in past observations, in underlying
297 processes, and understand how these are simulated by convection permitting
298 RCMs;
- 299 ● Explain major events in the context of climate change, via “storylines” of
300 individual events under different climatic conditions, but conditional on a fixed
301 state of the large-scale atmospheric circulation (e.g., Meredith et al., 2015;
302 Shepherd et al., 2014) in addition to a more robust assessment of uncertainties
303 using an ensemble-based approach;
- 304 ● Investigate life cycles of convective phenomena and related processes in the
305 context of a changing climate;

- 306 ● Identify the added-value of convection-permitting models in simulating such
307 trends with respect to standard resolution regional climate models, including the
308 investigation of relevant underlying processes;
- 309 ● Include additional processes/phenomena such as high altitude snow and related
310 hydro climatic impacts, mesoscale processes such as low-level wind convergence,
311 orographic interactions, land-atmosphere interactions and hydrological impacts;
- 312 ● Identify the added value of CP-RCM scenario simulation;

313

314 **2. Does an improved representation of convective processes and precipitation at**
315 **convection permitting scales lead to upscaled added value?**

316

- 317 ● How improved are CP-RCM aggregated precipitation statistics compared to
318 lower-resolution models up to the resolution of GCMs?
- 319 ● Do CP-RCMs and parameterized models have the same temperature-
320 precipitation intensity relation (as formulated in Lenderink & van Meijgaard,
321 2008)?
- 322 ● Can CP-RCMs serve as reference to improve convection parameterizations,
323 from shallow to deep?
- 324 ● Are there differences in the representation of key feedback processes between
325 parameterized and explicit convection (e.g. Hohenegger et al. 2009)?
- 326 ● Are there improvements in the aggregate statistics of other near-surface variables
327 such as temperature and wind?

328

329 **3. Is it possible to augment costly convection-permitting experiments with**
330 **physically defensible statistical downscaling approaches such as “convection**

331 **emulators” that mimic CP-RCMs and are fed by output of conventional-scale**
332 **RCMs?**

333

334 ● Can the variability of local-scale convective precipitation be sensibly predicted
335 by statistically downscaling 0.11° area-averages of variables that are typically
336 provided by RCMs?

337 ● Can the corresponding response to climate change be sensibly predicted by
338 corresponding 0.11° resolution RCM predictors?

339 ● Can statistical methods be advanced to include temporal discretization that
340 elucidates sub-daily rainfall;

341 ● Can these approaches be expanded to include temperature and wind?

342

343 *Expected impact*

344

345 ● Improved understanding of mechanisms and factors that influence location,
346 intensity, frequency and extent of convective precipitation events under changing
347 climate conditions;

348 ● Better constrained estimates of future changes in convective extremes and
349 associated processes, phenomena and feedbacks across Euro-Mediterranean
350 regions;

351 ● Bridge the spatial scale gap between regional climate models and impact models
352 (hydrological models, ecosystem models, etc.)

353 ● Provide added value for the decision-making process through analysis of risks
354 and opportunities associated with changes in extreme convective events.

355

356 *Timeline/Experiment Protocol*

357

358 *2017: First set of simulations:* RCM simulations will be run at convection-permitting
359 resolutions for selected test periods

- 360 ● Mandatory domain centered on the Alpine chain (1°-17° longitude East, 40°-50°
361 latitude North) (Figure 1);
- 362 ● Individual model sub-groups coordinate multi-physics options internally and
363 conduct short tests;
- 364 ● Perform test case study experiments with model systems run in weather like
365 (WL) and climate mode (CM), see Methods for more details.
- 366 ● Finalize the definition of the other FPS domains.

367

368 *2018: Begin ERA-Interim evaluation simulations*

369

- 370 ● Perform simulations that will systematically assess the ability of the CP-RCMs
371 to represent the present climate period chosen to overlap with recent high
372 resolution observation campaigns: 2000-2014 (minimum 10 years), ERA-Interim.
- 373 ● Develop a statistical convection model that will be employed to identify
374 mechanisms of long-term changes in convective precipitation and serve to
375 evaluate the representation of underlying processes, assess added value and
376 emulate convective precipitation.

377

378 *2019-2021: Third set of simulations, event interpretation, detailed analyses and*
379 *intercomparisons*

380

406 1. the weather like initialization (WL)

407 2. the climate mode initialization (CM)

408

409

410 For each case study ERA-Interim is used to provide boundary conditions (Dee et al., 2011).

411 Twenty of twenty-three modeling teams used the same nesting strategy, which was to nest

412 (one-way) the convection permitting domain within a 0.11 degree pan-European domain with

413 ERA-Interim driving the LBCs (see Table 1). This nesting procedure has been performed for

414 each of the modes (WL and CM) separately and exactly for the respective simulation period,

415 leading to different LBCs for CM respectively WL modes. However, teams were also

416 allowed freedom to pursue alternative nesting strategies, which could be used as departure

417 points for investigating the possibility for direct downscaling from e.g., ERA-Interim scales

418 to convection permitting scales and the effects of internal variability developing in the

419 intermediate domain. A few of the CCLM teams chose these different strategies, which

420 clearly impacted the results in interesting ways. One team (CCLM-5-0-9-JLU) directly

421 downscaled from ERA-Interim to ~3km for both simulations. Two others (CCLM-5-0-9-KIT

422 and COSMO-CMCC) first downscaled ERA-Interim to an intermediate pan-European

423 domain (0.22 degrees) for a long-term (> 15 years) and then used output from this for the

424 convection permitting simulations after the fact. These two approaches have the same net

425 effect, which is to impose identical lateral atmospheric boundary forcing for both the WL and

426 CM simulations. This tightly constrains the forcing at the lateral boundaries and should, in

427 principle, limit the development of internal variability.

428

429 For each modeling team WL and CM simulations follow the same nesting procedure,

430 however the WL experiments are initialized 24-48 hours before the HP event while the CM

431 ones are initialized one month before the event. The acronyms of the three case studies and
432 the initialization procedures are reported in Table 2 for both the WL and CM cases. This is
433 not meant to be a repetition of similar exercises carried out by the the NWP community
434 (though in this instance the ensemble is much larger than any previously aggregated). It is
435 rather intended as a first check of the ensemble and the individual models (especially new
436 ones) before the consortium launches into the planned long-term climate simulations. It is
437 worth noting that only a preliminary diagnostic analysis of the ensemble model performance
438 is presented here, and a full-fledged, detailed, evaluation of the results is out of the scope,
439 (which is presented in other papers of the special issue). The intention of this paper is
440 primarily to introduce the FPS, and to detail the approach, focusing on challenges and
441 potential.

442 **Preliminary results**

443 For each of the three test case studies and for both experiment configurations, the analysis
444 focuses here on the total accumulated precipitation for the whole domain during the event as
445 defined in Table 2 and on the time series of hourly and 12 hours accumulated precipitation in
446 the region of maximum precipitation as indicated by observations.

447

448 Case 1

449 The first case (Case 1), referred to as HyMeX-IOP16 (Intense Observation Period 16) in
450 Table 2, is a HP event occurred during the HyMeX measurement campaign in September-
451 November 2012 (Ducrocq et al. 2014). The event is documented in detail by Duffourg et al.,
452 (2016) and Martinet et al., (2017), and it consists of slow propagating mesoscale convective
453 systems (MCSs) associated with the evolution of a trough interacting with an upper-level low
454 centered over the Iberian Peninsula which induced warm, moist and unstable southerly flow
455 in the lower troposphere over the western Mediterranean. The interaction of the upper-level

456 forcing with the warm low-level air mass increased instability and induced the deepening of a
457 depression over the Gulf of Lion, favoring in turn the formation of MCSs that affected
458 Southern France and Northern Italy between 25 and 27 Oct, 2012. According to the station
459 observations collected during the field campaign (Ducrocq et al., 2014, <http://hoc.sedoo.fr> for
460 HyMeX database) three regions were mainly affected by heavy precipitation. Two areas
461 were in Southern France - referred to as CV1 and CV2 and indicating, respectively, the
462 western and eastern parts of the Cévennes-Vivarais (CV) observation site during the HyMeX
463 campaign (see Figure 1 in Ducrocq et al., 2014). The third affected area was Liguria-Tuscany
464 one (LT, Figure 1 in Ducrocq et al., 2014). These three regions are highlighted in Figure 2a
465 with red, green and blue squares; here the observed total accumulated precipitation maxima
466 were, respectively, around 170, 140, and 250 mm. The same figure shows the ensemble
467 average of the WL and CM experiments in panels b and c, respectively, along with all the
468 individual ensemble members (WL/CM in the left/right columns).

469

470 As a general comment, we can observe how the locations of the three maxima are generally
471 well captured by the WL ensemble, although the precipitation intensities are lower than
472 observed. For the CM ensemble, the average location of the three events is still well
473 represented but the underestimation is more pronounced. This ensemble behavior is reflected
474 in the individual realizations, where for each CM simulation the intensity of maximum
475 precipitation is lower than the corresponding WL one, although some members of the
476 ensemble still show a maximum precipitation higher than observed.

477

478 A more quantitative analysis is reported in Table 3, where for each model and for both modes
479 the spatial correlation of the total accumulated precipitation in the 3 boxes is computed
480 between the observed interpolated field (Figure 2a2) and the model output. If we consider a

481 threshold of 0.5 for a reasonable correlation score, 60% of the WL simulations in the CV1
482 regions have a correlation higher than 0.5, 30% in CV2 and 20% in LT regions. For the CM
483 simulation the percentages drop to 23% and 14% in the first two regions but increase to 57%
484 in the LT regions.

485 In Figures 3a,d, and g the spatial correlation of the 12 hourly accumulated precipitation is
486 reported over the duration of the event for each model and for both WL and CM simulations.
487 The value of the observed 12 hourly accumulated precipitation is reported too, as an
488 indication of the time evolution of the event across the 3 regions. For each box the peak
489 model skill is reached during the peak of the event and the percentage of models that are
490 above 0.5 correlation value remains similar to those reported in Table 3 as does the ratio
491 between CM and WL. These indicate that the ability of the models to follow the time
492 evolution of the event is similar in both WL and CM mode.

493

494 Concerning the timing and intensity of the events in the 3 subregions, the hourly accumulated
495 precipitation averaged over each box is plotted for each WL and CM ensemble member in
496 Figures 3b,e, and h, along with the observations and the WL and CM ensemble average value
497 in panels c, f and i. For the CV1 and LT regions the WL and CM ensembles behave in the
498 same way, both showing a delay in the onset of the event and an underestimation of the peak
499 intensity. The simulated intensity is higher for the WL than the CM, consistently with what is
500 observed in Figure 2. For the CV2 region, both the WL and CM ensembles exhibit the same
501 time delay and similar peak precipitation underestimations.

502

503 Case 2

504

505 Case 2 (called AUSTRIA hereafter) is a convective orographic precipitation event with weak
506 but persistent large-scale driving factors that was induced by the evolution of a shallow
507 trough over the North Atlantic, from 22-25 June 2009. A cutoff low was isolated over
508 Southern Europe, thus inducing persistent northeasterly flow over Austria, associated with
509 unstable warm-moist air, impinging on the Alps. This caused extreme rainfall along the
510 northern flanks of the Alps due to orographic lifting. On June 24, however, the position of the
511 rainfall maximum moved further to the east and south (Burgenland and South-Eastern Styria)
512 because of strong embedded deep-convective cells (Haiden, 2009). On June 25, the
513 regionally extended event ended and became more localised and scattered. The overall largest
514 6-day (22-27June) rainfall sum was recorded at station Steinholz (lower Austria, located in
515 the northern foothills of the Eastern Alps) with 354 mm and a return period of more than 100
516 years (Godina and Müller, 2009).

517

518 In Figure 4 the same analysis as Figure 2 is reported but for Case 2 precipitation. The
519 observed precipitation (Figure 4a) shows a hook-shaped spatial pattern with the highest
520 maxima following the terrain elevation peaks and a secondary maximum in the southeastern
521 part of the domain. The WL ensemble (Figure 4b1) shows a less pronounced hook shape
522 precipitation, with the first maximum well located but with lower intensity than observed and
523 with the secondary maximum definitely underestimated. These translate in a percentage of
524 90% of the models that have a spatial correlation pattern of the total accumulated
525 precipitation higher than 0.5 (see Table 4). The CM ensemble (Figure 4b2) reduces even
526 more this signal up to a 60% underestimation of the maximum value. In contrast to the
527 previous case study, the CM ensemble value is the result of a few CM members capturing the
528 event and even overestimating it, a few showing different spatial pattern distributions from
529 observed and half of the ensemble members not capturing or severely underestimating it as it

530 is confirmed from the drop of the percentage of models with good correlation score to only
531 42% (see Table 4). Also in this case the skill in following the time evolution of the events is
532 maximum during the pick of the precipitation and the evolution in time of the skill for both
533 WL and CM mode (Figure 5a) and is consistent with Table 4.

534

535 This large uncertainty is well depicted in Figure 5b, where the hourly accumulated
536 precipitation averaged over the rectangular box in Figure 4a is reported as a function of time.
537 The individual CM ensemble members go from nearly zero mm to over 1.5 times the
538 observed accumulation, while the WL ensemble members are more narrowly grouped around
539 the observed accumulation line. The difference in behaviour between the two ensembles is
540 evident in Figure 5c where the CM ensemble shows an underestimation around the 60% of
541 the correspondent observed curve and in accordance with Figure 4.

542

543 Case 3

544 Case 3 (called FOEHN hereafter) is a Foehn event that occurred on November 2014 Kramer
545 et al., 2017). In this case the slow eastward evolution of a deep trough, associated with a mid-
546 latitude cyclone over the North Atlantic induced persistent southerly flow over the Alps.
547 Steady orographic precipitation occurred on the windward side of the Alps, with a consequent
548 release of latent heat and drying of the air, that induced a Foehn effect on the leeward side of
549 the mountains. The slow eastward evolution of the trough caused persistent precipitation over
550 the Alps with daily precipitation locally exceeding several hundreds of mm and reaching
551 maxima around 500 mm. From Figure 6a-b we can see that both the WL and CM ensembles
552 agree well with observations. All the single members of the WL and CM have a similar
553 behavior, the spatial correlation of the total accumulated precipitation is above 70% in both
554 cases (see Table 5), the time evolution of the models skill is similar among the WL and CM

555 and is always very high (above 0.5 for most of the event) as it is shown in Figure 7a, the
556 maximum intensity is reproduced and the hourly evolution of the event is well captured
557 (Figure 7a). The model spread is symmetric around the observations and the ensemble
558 average WL and CM precipitation amounts are in good agreement with the observations both
559 in terms of timing and magnitude.

560 **Discussion**

561 In this manuscript we have introduced an ambitious, first-of-its-kind project that aims to
562 design, produce and analyze multi-model ensembles of CP simulations. The project is
563 organized under the WCRP-sponsored CORDEX - Flagship Pilot Studies mechanism. As
564 such, the project mobilizes participants from Euro-CORDEX, Med-CORDEX and
565 CORDEX-ESD (Empirical Statistical Downscaling). The project has also engaged actors
566 from outside the CORDEX community in order to bring in fresh perspectives and additional
567 expertise. This diverse consortium is able to leverage years of expertise in NWP, climate
568 modeling and downscaling, statistical modeling and downscaling. The overarching scientific
569 aim of the project is to produce long-term simulations under present and future conditions at
570 CP resolutions, with focus on increasing our understanding of convection, convective
571 processes and their impacts in a global warming context. Given the challenges and costs
572 involved in running dynamical models at CP-RCM scales, test cases were designed to
573 provide a zero-order assessment of the ensemble and its characteristics. In this manuscript we
574 have presented a preliminary and illustrative analysis of these case studies.

575

576 These preliminary results of the three case studies illustrate both the challenges and potential
577 in CP-RCMs. They also provide a clear argument for the advantages of the ensemble-based
578 approach. Case 1 is a fall HP event driven by the development of MCS over the western
579 Mediterranean basin advecting moist air over three topographically complex regions in the

580 southern coast of France and the Liguria-Tuscany regions. The three precipitation maxima
581 are well located by both WL and CM ensembles. However, the intensity of the peaks is
582 generally underestimated, especially in the CM experiments. Case 2 is an orographic
583 precipitation event that shows the effects of internal variability more strongly in CM than the
584 other cases. From the ensemble point of view the event is captured in both WL and CM
585 mode, with the latter one showing much more damped signals. The Foehn case (Case 3) is
586 characterized by persistent orographic precipitation driven by a slow eastward moving
587 through and it was the best captured by the models. Both the WL and CM ensembles were in
588 very good agreement with observations, representing well both the timing and intensity of the
589 HP event.

590

591 There are interesting and subtle differences between the case studies themselves and the ways
592 in which the individual models represent them. Even within an individual test case there are
593 differences in dominant processes that are then reflected by the ensemble. The general
594 increase in spread (both spatially and temporally) between the WL and CM can be expected
595 and points toward the strong effect of internally generated variability in the models.

596

597 Case 1 shows a larger spread over regions in which the precipitation is most affected by
598 complex topography. Unsurprisingly, the individual WL and CM ensemble members exhibit
599 a broader range of behaviors over these areas (the red and blue boxes in Figure 2), which
600 results in different ensemble mean responses. Conversely, the model behaviour is more
601 consistent between WL and CM over the CV2 region (green box), resulting in very similar
602 ensemble mean responses and correlation skill score of the individual models (Table 3 and
603 Figure 3d). The heavy precipitation event over this area was the result of an organized MCS
604 forming over the sea, weakly supported by the orographic forcing. In this case the WL

605 simulations are closer to the CM behaviour on average (low predictability problem), with
606 some members showing results as uncertain as in CM.

607

608 Case 2 is in many ways the most interesting, with a wide range of model behaviours in the
609 CM simulations. Some simulations completely miss the event while others exhibit a
610 considerably damped response. Only 9 of the 21 CM simulations have the spatial pattern of
611 the total accumulated rainfall that has a correlation with the observations higher than 0.5
612 (Table 4). While one should not expect exact reproduction of events in terms of timing,
613 location and intensity in CM, it is reasonable to expect credible representation of the events
614 given the experiment design. Therefore we provide some discussion on why some models
615 reproduced the salient characteristics of the event over Austria whereas some missed it
616 entirely. A detailed investigation is beyond the scope of this paper, but we speculate that at
617 least three factors may be responsible for this result. The first is that the event is close to the
618 domain boundaries, which can be problematic, and model teams used varying sponge layer
619 depths and nesting strategies. This last point is illustrated by the fact that the simulations that
620 missed the event in its entirety all had an freely evolving (i.e. not nudged) intermediate nest,
621 which allows internal variability to develop. Interestingly, the differences in nesting strategy
622 did not have such a strong effect on the other test cases. Another factor is that this event
623 occurred in a relatively weak background synoptic state, which would decrease the large
624 scale forcing compared to the local forcing, and thus increase diversity across models. Lastly,
625 though the spread is large, the ensemble mean pattern captures the event, and the location of
626 each simulations' maximum rainfall is roughly in the correct region (i.e. along the Northern
627 foothills of the Austrian Alps, not shown). This can be considered as a good starting point for
628 a future analysis where a more in depth investigation will be needed to fully understand the
629 driver of the HP event and the reason some of the models do not capture it.

630

631 Case 3 showed the best model performance in both the WL and CM ensembles. In this
632 experiment, both the ensemble mean and all individual members reproduce the results, in
633 terms of precipitation, of a strong Foehn event. The reason for this could be that this event is
634 driven by a well-defined, slowly-evolving large-scale circulation which forced long-lasting
635 orographic precipitation over the Alps. It is worth mentioning that this case presents the
636 typical synoptic conditions conducive to heavy Alpine rainfall, which are easier to predict
637 than average conditions (Grazzini, 2007). Therefore, models which are able to capture the
638 large scale organization of the precipitating system can provide a quite surprising
639 reproduction of the event, provided that convective precipitation, embedded in the stratiform
640 rainfall, is represented.

641

642 The preliminary results presented here have important implications for the longer term
643 simulations the project aims to undertake, and more generally for the use of CP-RCM in a
644 climate context; one is that results can be highly model and event dependent. They suggest
645 that we can expect varying ranges of responses for different types of convective events (e.g.
646 strongly steered by synoptic conditions vs. weakly steered, local scale interactions with
647 complex topography vs. stronger ocean influence, etc.), which would affect uncertainties in
648 future projections. As Grell et al. (2000) noted, precipitation over complex terrain is not
649 likely to converge toward one solution at CP-RCM scales and, more importantly, the
650 precipitation moves with the local upper level flow unlike in coarser RCM simulations where
651 the precipitation remains locked to the mountain tops. For test cases, however, it is difficult to
652 disentangle the extent to which model differences are due to internal noise (which will lead to
653 differences in the timing, positioning and evolution of specific event, particularly if not
654 strongly forced by the large-scale conditions) or due to differences in model physics. Multi-

655 year climatological statistics will be less influenced by internal noise and hence the
656 intercomparison of results from the upcoming ERA-Interim (and scenario) simulation across
657 models will allow a more in depth understanding of model performance and uncertainty. For
658 more insight on some of the issues raised here, the authors would like to point the reader to
659 the other papers in the special collection convection permitting modeling.

660

661 The CORDEX-FPS on convection over Europe and the Mediterranean is an ambitious and
662 challenging undertaking. It has a tremendous potential and is a logical next step to bring
663 together the Euro-CORDEX, Med-CORDEX and the nascent scientific communities forming
664 around the use of CP-RCM on climate scales. The findings from the project will enhance our
665 understanding of convective processes and their response to climate warming, which may
666 bring some surprises with respect to the findings from coarse resolution models (e.g. Giorgi
667 et al. 2016). Further, as recent single model, longer-term climate change CP-RCM
668 experiments indicate, previously unresolved but highly destructive features such as intense
669 mesoscale convective systems increase substantially in a warming climate (Prein et al. 2017).
670 The project will, therefore, also provide critical added value to decision makers as ensemble-
671 based and combined dynamical-statistical approaches will help improve confidence even
672 under conditions of high uncertainty. The initiative is open to all interested scientists and
673 potential collaborators are encouraged to contact the project leaders if they wish to
674 participate.

675 **Acknowledgements**

676 I.G. and L.S. have been supported by the Croatian Science Foundation (HrZZ) project CARE
677 (no. 2831). J.F. acknowledges support by the Spanish R+D programme through
678 MINECO/FEDER co-funded project INSIGNIA (CGL2016-79210-R). A.L-G. is supported
679 by the Spanish government through grant BES-2016-078158 and MINECO/FEDER co-

680 funded project MULTI-SDM (CGL2015-66583-R). UCAN simulations have been carried out
681 on the Altamira Supercomputer at the Instituto de Física de Cantabria (IFCA, CSIC-UC),
682 member of the Spanish Supercomputing Network. Computational resources were partly made
683 available by the German Climate Computing Center (DKRZ) through support from the
684 BMBF. J.M. and K.W.-S. gratefully acknowledge the support by the German Science
685 Foundation (DFG) through project FOR 1695. UHOH simulations were carried out at the
686 supercomputing center HLRS in Stuttgart, Germany. D.M., M.P., and H.T. gratefully
687 acknowledge the support received via the Austrian Science Fund (FWF) project NHCM-2
688 (no. P24758-N29) and the projects HighEnd:Extremes and EASICLIM, funded by the
689 Austrian Climate Research Programme (ACRP) of the Klima- und Energiefonds (no.
690 KR13AC6K10981 and KR16AC0K13160, respectively). D.M., M.P. and H.T. are also
691 thankful for the computational resources received the Vienna Scientific Cluster (VSC). K.G.,
692 S.K., H.T. and M.P. gratefully acknowledge the computing time granted by the John von
693 Neumann Institute for Computing (NIC) and provided on the supercomputer JURECA at
694 Jülich Supercomputing Centre (JSC) through grant hka19. D.H. gratefully acknowledges the
695 Gauss Centre for Supercomputing e.V. (www.gauss-centre.eu) for funding this project by
696 providing computing time on the GCS Supercomputer JUQUEEN at Jülich Supercomputing
697 Centre (JSC) through grant hka19. S.S. and T.L. acknowledge the support of NOTUR
698 project no. NN9280K and the Research Council of Norway and its basic institute support of
699 their strategic project on Climate Services. The authors gratefully acknowledge the Austrian
700 Central Department for Meteorology and Geodynamics (ZAMG) for providing analysis fields
701 of the Integrated Nowcasting through Comprehensive Analysis (INCA) system. IPSL's work
702 was granted access to the HPC resources of TGCC under the allocations 2017-A0010106313
703 and 2017-A0030106877 made by GENCI. RMC and PMMS gratefully acknowledge the
704 support of the SOLAR project (PTDC/GEOMET/7078/2014) financed by the Portuguese

705 Foundation for Science and Technology. Q.F. and S.S. acknowledge the support of the
706 Meteo-France computing center and warmly thank Antoinette Alias and Michel Déqué for
707 their contributions. E.J. Kendon gratefully acknowledges funding from the Joint Department
708 of Energy and Climate Change (DECC) and Department for Environment Food and Rural
709 Affairs (Defra) Met Office Hadley Centre Climate Programme (GA01101). S. Khodayar
710 research is supported by the Bundesministerium für Bildung und Forschung (BMBF; German
711 Federal Ministry of Education and Research). E.K. and S.K. acknowledge the support of the
712 Greek Research and Technology Network (GRNET) High Performance Computing (HPC)
713 infrastructure for providing the computational resources of AUTH-simulations and the
714 AUTH Scientific Computing Center for technical support. T.H. and M.B. (CUNI)
715 acknowledge the support of the IT4Innovations - National Supercomputer Centre of the
716 Czech Republic providing the computational resources for the CUNI simulations and the
717 support of Ministry of Education, Youth and Sports of the Czech Republic for funding the
718 participation in Euro-CORDEX activities via the scheme INTER-TRANSFER under the
719 grant No. LTT17007. L.M., G.M. and Ø.H. acknowledge supercomputer facilities provided
720 by NOTUR, and funding from the Research Council of Norway through the SUPER (grant
721 no. 250573) and HYPRE (grant no. 243942) projects. HCLIM-KNMI simulations were
722 supported by ECMWF (computing time through special project SPNLSTER) and the Dutch
723 Ministry of Infrastructure and the Environment. H.d.V. and E.v.M. like to thank Bert van Uft
724 from KNMI for carrying out the Harmonie simulations.

725 ICTP thanks the CINECA super computer center for the HPC facilities used for those
726 simulations.

727 The authors also wish to thank MeteoGroup Switzerland for providing observational data for
728 the Foehn test case, Meteo-France and the HyMeX program (sponsored by Grants
729 MISTRALS/HyMeX and ANR-11-BS56-0005 IODA-MED project) for supplying the data

730 for HyMeX-IOP16 case, the Wegener Center (especially Jürgen Fuchsberger) for providing
731 WegenerNet data for the Austria case.

732

733

734 **References**

735 Ahrens, B., Jasper, K., and Gurtz, J. (2003) On ALADIN Precipitation Modeling and
736 Validation in an Alpine Watershed. *Annales Geophysicae* 21:627–637

737

738 Argüeso, D., Evans, J.P., Fita, L. and Bormann, K.J. (2014) Temperature response to future
739 urbanization and climate change. *Climate dynamics* 42(7-8):2183-2199.

740

741 Ban, N., J. Schmidli, and C. Schär (2014) Evaluation of the convection-resolving regional
742 climate modeling approach in decade-long simulations. *J. Geophys. Res. Atmos.* 119: 7889–
743 7907. doi:10.1002/2014JD021478.

744

745 Ban, N., Schmidli, J. and Schär, C. (2015) Heavy precipitation in a changing climate: Does
746 short-term summer precipitation increase faster? *Geophys. Res. Lett.* 42: 1165–1172. doi:
747 10.1002/2014GL062588.

748

749 Beaulant, A.-L., B. Joly, O. Nuissier, S. Somot, V. Ducrocq, A. Joly, F. Sevault, M. Deque &
750 Ricard, D. (2011) Statistico-dynamical downscaling for Mediterranean heavy precipitation.

751 *Q. J. Royal Meteorol. Soc* 137:736-748

752

753 Beniston, M. (2006) August 2005 intense rainfall event in Switzerland: Not necessarily an
754 analog for strong convective events in a greenhouse climate. *Geophys. Res. Lett.*
755 *33(5):L05701. doi:10.1029/2005GL025573*
756

757 Benoit, R., Schaer, C., Binder, P., Chamberland, S., Davies, H. C., Desgagne', M., Girard, C.,
758 Keil, C., Kouwen, N., Luethi, D., Maric, D., Mueller, E., Pellerin, P., Schmidli, J., Schubiger,
759 F., Schwierz, C., Sprenger, M., Walser, A., Willemsse, S., Yu, W., and Zala, E. (2002) The
760 real-time ultra finescale forecast support during the special observing period of the MAP,
761 *Bull. Amer. Meteor. Soc.* 83:85–109.
762

763 Bollmeyer, C. et al (2015) Towards a high-resolution regional reanalysis for the European
764 CORDEX domain. *Q. J. Royal Meteorol. Soc.* 141(686):1–15, doi:10.1002/qj.2486.
765

766 Bony, S., Stevens, B., Frierson, D.M., Jakob, C., Kageyama, M., Pincus, R., Shepherd, T.G.,
767 Sherwood, S.C., Siebesma, A.P., Sobel, A.H. and Watanabe, M. (2015) Clouds, circulation
768 and climate sensitivity. *Nature Geoscience*, 8(4):261-268.
769

770 Brisson, E., Van Weverberg, K., Demuzere, M., Devis, A., Saeed, S., Stengel, M. and van
771 Lipzig, N.P. (2016) How well can a convection-permitting climate model reproduce decadal
772 statistics of precipitation, temperature and cloud characteristics? *Climate Dynamics* 47(9-
773 10):3043-3061.
774

775 Carvalho, L.M., Jones, C. and Liebmann, B. (2002) Extreme precipitation events in
776 southeastern South America and large-scale convective patterns in the South Atlantic
777 convergence zone. *Journal of Climate* 15(17):2377-2394.

778

779 Chen, S. S. et al. (2016) Aircraft observations of dry air, the ITCZ, convective cloud systems,
780 and cold pools in MJO during DYNAMO. *Bull. Amer. Meteor. Soc.* 97:405–423.
781 doi:<https://doi.org/10.1175/BAMS-D-13-00196.1>

782

783 Davis, C., B. Brown, and R. Bullock (2006) Object-based verification of precipitation
784 forecasts: Part II. Application to convective rain systems, *Mon. Weather Rev.* 134(7):1785–
785 1795. doi: [10.1175/MWR3146.1](https://doi.org/10.1175/MWR3146.1).

786

787 Dee, D. P., Uppala, S. M., Simmons, A. J., Berrisford, P., Poli, P., Kobayashi, S., ... &
788 Bechtold, P. (2011). The ERA-Interim reanalysis: Configuration and performance of the data
789 assimilation system. *Quarterly Journal of the royal meteorological society*, 137(656), 553-
790 597.

791

792 Déqué M., Alias A., Somot S., Nuissier O. (2016) Climate change and extreme precipitation:
793 the response by a convection-resolving model. Research activities in atmospheric and oceanic
794 modelling. CAS/JSC Working group on numerical experimentation. Report No.46.
795 http://www.wcrp-climate.org/WGNE/blue_book.html. Accessed 5 December 2017

796

797 Delrieu, G., Wijbrans, A., Boudevillain, B., Faure, D., Bonnifait, L., & Kirstetter, P. E.
798 (2014) Geostatistical radar–raingauge merging: a novel method for the quantification of rain
799 estimation accuracy. *Advances in Water Resources* 71:110-124.

800

801 Deser, C., Phillips, A., Bourdette, V. and Teng, H. (2012) Uncertainty in climate change
802 projections: the role of internal variability. *Climate Dynamics* 38(3-4):527-546.

803

804 Deser, C., Phillips, A.S., Alexander, M.A. and Smoliak, B.V. (2014) Projecting North
805 American climate over the next 50 years: Uncertainty due to internal variability. *Journal of*
806 *Climate* 27(6):2271-2296.

807

808 Dirmeyer, P.A., Cash, B.A., Kinter, J.L., Jung, T., Marx, L., Satoh, M., Stan, C., Tomita, H.,
809 Towers, P., Wedi, N. and Achuthavarier, D. (2012) Simulating the diurnal cycle of rainfall in
810 global climate models: Resolution versus parameterization. *Climate dynamics* 39(1-2):399-
811 418.

812

813 Done, J., C. A. Davis, and M. Weisman (2004) The next generation of NWP: Explicit
814 forecasts of convection using the Weather Research And Forecasting (WRF) model. *Atmos.*
815 *Sci. Lett.* 5(6):10–117.

816

817 Drobinski P, Ducrocq V, Alpert P, Anagnostou E, Beranger K, Borga M, Braud I, Chanzy A,
818 Davolio S, Delrieu G, Estournel C, Filali Boubrahmi N, Font J, Grubisic V, Gualdi S, Homar
819 V, Ivancan-Picek B, Kottmeier C, Kotroni V, Lagouvardos K, Lionello P, Llasat MC,
820 Ludwig W, Lutoff C, Mariotti A, Richard E, Romero R, Rotunno R, Roussot O, Ruin I,
821 Somot S, Taupier-Letage I, Tintore J, Uijlenhoet R, Wernli H. (2014). HyMeX, a 10- year
822 multidisciplinary program on the Mediterranean water cycle. *Bull. Am. Meteorol. Soc.* 95:
823 1063–1082. <https://doi.org/10.1175/BAMS-D-12-00242.1>

824

825 Ducrocq V, Ricard D, Lafore JP, Orain F. (2002) Storm-scale numerical rainfall prediction
826 for five precipitating events over France: On the importance of the initial humidity field.
827 *Weather and Forecasting* 17:1236–1256.

828

829 Ducrocq V, Nuissier O, Ricard D, Lebeauvin C, Thouvenin T (2008) A numerical study of
830 three catastrophic precipitating events over southern france. ii: Mesoscale triggering and
831 stationarity factors. Quarterly journal of the royal meteorological society 134(630):131–145

832

833 Ducrocq V, Braud I, Davolio S, Ferretti R, Flamant C, Jansa A, Kalthoff N, Richard E,
834 Taupier-Letage I, Ayrat PA, Belamari S, Berne A, Borga M, Boudevillain B, Bock O,
835 Boichard JL, Bouin MN, Bousquet O, Bouvier C, Chiggiato J, Cimini D, Corsmeier U,
836 Coppola L, Cocquerez P, Defer E, Drobinski P, Dufournet Y, Fourrie N, Gourley JJ, Labatut
837 L, Lambert D, Le Coz J, Marzano FS, Molinie G, Montani A, Nord G, Nuret M, Ramage K,
838 Rison B, Roussot O, Said F, Schwarzenboeck A, Testor P, Van Baelen J, Vincendon B, Aran
839 M (2014) HyMeX-SOP1: The field campaign dedicated to heavy precipitation and flash
840 flooding in the northwestern Mediterranean. Bulletin of the American Meteorological Society
841 95(7):1083-1100.

842

843 Duffourg F, Nuissier O, Ducrocq V, Flamant C, Chazette P, Delanoë J, Doerenbecher A,
844 Fourrié N, Di Girolamo P, Lac C, et al (2016) Offshore deep convection initiation and
845 maintenance during the hymex iop 16a heavy precipitation event. Quarterly Journal of the
846 Royal Meteorological Society 142(S1):259–274

847

848 Fosser, G., S. Khodayar, and P. Berg (2014) Benefit of convection permitting climate model
849 simulations in the representation of convective precipitation, Clim. Dyn. 44(1– 2):45–60.

850

851 Giorgi, F., C. Jones, and G. R. Asrar (2009), Addressing climate information needs at the
852 regional level: the CORDEX framework, WMO Bulletin 58(3):175-183.

853

854 Giorgi, F., C. Torma, E. Coppola, N. Ban, C. Schar and S. Somot (2016) Enhanced summer
855 convective rainfall at Alpine high elevations in response to climate warming. *Nat. Geosci.* 9:
856 584-589.

857

858 Godina, R. and Müller, G. (2009) Das Hochwasser in Österreich vom 22. bis 30 Juni, 2009 –
859 Beschreibung der hydrologischen Situation (in German), Report, pp 21, Austrian Federal
860 Ministry of Agriculture, Forestry, Environment and Water Management (BMLFUW), Abt.
861 VII/3., Vienna, Austria. <https://www.bmlfuw.gv.at/wasser/wasser->

862 [oesterreich/wasserkreislauf/hydrograph_charakt_extrema/Hochwasser-Juni2009.html](https://www.bmlfuw.gv.at/wasser/wasser-oesterreich/wasserkreislauf/hydrograph_charakt_extrema/Hochwasser-Juni2009.html).

863 Accessed 5 December 2017

864

865 Grazzini F. (2007) Predictability of a large-scale flow conducive to extreme precipitation
866 over the western Alps. *Met. Atm. Phys.* 95:123-138.

867

868 Grell, G. A., L. Schade, R. Knoche, A. Pfeiffer, and J. Egger (2000) Nonhydrostatic climate
869 simulations of precipitation over complex terrain, *J. Geophys. Res.* 105(D24): 29595–29608.

870

871 Gutowski Jr, W. J., Giorgi, F., Timbal, B., Frigon, A., Jacob, D., Kang, H. S., Raghavan, K.,
872 Lee, B., Lennard, C., Nikulin, G., O'Rourke, Rixen, M., Solman, S., Stephenson, T., and
873 Tangang, F. (2016) WCRP COordinated Regional Downscaling EXperiment (CORDEX): a
874 diagnostic MIP for CMIP6, *Geosci. Model Dev.* 9:4087–4095.

875 <https://doi.org/10.5194/gmd-9-4087-2016>

876

877 Haiden, T., A. Kann, C. Wittmann, G. Pistotnik, B. Bica, and C. Gruber (2011), The
878 Integrated Nowcasting through Comprehensive Analysis (INCA) System and Its Validation
879 over the Eastern Alpine Region, *Wea. Forecasting* 26(2):166-183, doi:
880 10.1175/2010WAF2222451.1

881

882 Hawkins, E. and Sutton, R. (2009) The potential to narrow uncertainty in regional climate
883 predictions. *Bulletin of the American Meteorological Society*, 90(8):1095-1107.

884

885 Heinzeller, D., Junkermann, W., Kunstmann, H. (2016) Anthropogenic Aerosol Emissions
886 and Rainfall Decline in Southwestern Australia: Coincidence or Causality? *J. Climate* 29:
887 8471-8493. doi: 10.1175/JCLI-D-16-0082.1

888

889 Hohenegger, C., P. Brockhaus, C.S. Bretherton and C. Schär (2009) The soil moisture-
890 precipitation feedback in simulations with explicit and parameterized convection. *J. Clim.* 22
891 (19):5003–5020.

892

893 Holloway, C. E., and J. D. Neelin, (2009) Moisture vertical structure, column water vapor,
894 and tropical deep convection. *J. Atmos. Sci.* 66:1665–1683.

895

896 Jakob, M. and Weatherly, H. (2003) A hydroclimatic threshold for landslide initiation on the
897 North Shore Mountains of Vancouver, British Columbia. *Geomorphology* 54(3):137-156.

898

899 Kendon, E.J., Roberts, N.N., Senior, C.A., & Roberts, M.J. (2012) Realism of Rainfall in a
900 Very High-Resolution Regional Climate Model. *J. Climate* 25:5791–5806. doi:
901 <http://dx.doi.org/10.1175/JCLI-D-11-00562.1>

902

903 Kendon, E. J., Roberts, N. M., Fowler, H. J., Roberts, M. J., Chan, S. C., & Senior, C. A.
904 (2014). Heavier summer downpours with climate change revealed by weather forecast
905 resolution model. *Nature Climate Change* 4(7):570-576.

906

907 Khairoutdinov MF, Randall D. (2006) High-resolution simulation of shallow to deep
908 convection transition over land. *J. Atmos. Sci.* 63:3421–3436.

909

910 Khodayar S., G. Fosser, B. Segolene, S. Davolio, P. Drobinski, V. Ducrocq, R. Ferretti, M.
911 Nuret, E. Pichelli, E. Richard (2016) A seamless weather-climate multi-model
912 intercomparison on the representation of high impact weather in the Western Mediterranean:
913 HyMeX IOP12. *Q. J. R. Meteorol. Soc.* 142:433-452. doi: 10.1002/qj.2700

914

915 Klein, S. A., Y. Zhang, M. D. Zelinka, R. Pincus, J. Boyle, and P. J. Gleckler (2013) Are
916 climate model simulations of clouds improving? An evaluation using the ISCCP simulator. *J.*
917 *Geophys. Res. Atmos.*, 118:1329–1342. doi:10.1002/jgrd.50141.

918

919 Kramer, M., Heinzeller, D., Hartmann, H., van den Berg, W., Steeneveld, GJ. (2017)
920 Numerical Weather Prediction in the grey zone using a global variable resolution mesh and
921 scale-aware convection parameterisation using MPAS. Submitted to *Climate Dynamics*

922

923 Lenderink, G. & van Meijgaard, E. (2008) Increase in hourly precipitation extremes beyond
924 expectations from temperature changes. *Nature Geoscience* 1(8):511-514.
925 doi:10.1038/ngeo262.

926

927 Llasat, M. C., Llasat-Botija, M., Petrucci, O., Pasqua, A. A., Rosselló, J., Vinet, F., &
928 Boissier, L. (2013) Towards a database on societal impact of Mediterranean floods within the
929 framework of the HYMEX project. *Natural Hazards and Earth System Science*, 13(5): 1337-
930 1350.

931

932 Mass, C.F., D. Ovens, K. Westrick, and B.A. Colle (2002) Does Increasing Horizontal
933 Resolution Produce More Skillful Forecasts? *Bulletin of the American Meteorological*
934 *Society*, 83(3):407-430.

935

936 Maraun, D., Shepherd, T.G., Widmann, M., Zappa, G., Walton, D., Gutiérrez, J.M.,
937 Hagemann, S., Richter, I., Soares, P.M., Hall, A. and Mearns, L.O. (2017) Towards process-
938 informed bias correction of climate change simulations. *Nature Climate Change*, 7(11):764-
939 773.

940

941 Martinet M, Nuissier O, Duffourg F, Ducrocq V, Ricard D (2017) Fine-scale numerical
942 analysis of the sensitivity of the hymex iop16a heavy precipitating event to the turbulent
943 mixing length parameterization. *Quarterly Journal of the Royal Meteorological Society*.
944 doi:10.1002/qj.3167

945

946 Meredith, E. P., V. A. Semenov, D. Maraun, W. Park, and A. V. Chernokulsky (2015)
947 Crucial role of Black Sea warming in amplifying the 2012 Krymsk precipitation extreme.
948 *Nature Geoscience* 8:615-619. doi: 10.1038/NGEO2483.

949

950

951 Milovac, J., K. Warrach-Sagi, A. Behrendt, F. Späth, J. Ingwersen, and V. Wulfmeyer (2016)
952 Investigation of PBL schemes combining the WRF model simulations with scanning water
953 vapor differential absorption lidar measurements. *J. Geophys. Res. Atmos.* 121:624–649.
954 doi:10.1002/2015JD023927.

955

956 Najac, J., Lac, C., & Terray, L. (2011) Impact of climate change on surface winds in France
957 using a statistical-dynamical downscaling method with mesoscale modelling. *International*
958 *Journal of Climatology* 31(3):415-430.

959

960 Nester, T., R. Kirnbauer, D. Gutknecht, and G. Bloeschl (2011) Climate and catchment
961 controls on the performance of regional flood simulations. *Journal of Hydrology* 402(3-
962 4):340-356. doi: 10.1016/j.jhydrol.2011.03.028

963

964 Pontoppidan, M., Reuder, J., Mayer, S. and Kolstad, E.W. (2017) Downscaling an intense
965 precipitation event in complex terrain: the importance of high grid resolution. *Tellus A:*
966 *Dynamic Meteorology and Oceanography*, 69(1):1271561.

967

968 Prein, A., A. Gobiet, M. Suklitsch, H. Truhetz, N. Awan, K. Keuler, and G. Georgievski
969 (2013a) Added value of convection permitting seasonal simulations. *Clim. Dyn.* 41(9–
970 10):2655–2677.

971

972 Prein, A. F., Liu, C., Ikeda, K., Trier, S. B., Rasmussen, R. M., Holland, G. J., & Clark, M. P.
973 (2017). Increased rainfall volume from future convective storms in the US. *Nature Climate*
974 *Change*, 7(12), 880.

975

976 Prein, A. F., G. J. Holland, R. M. Rasmussen, J. Done, K. Ikeda, M. P. Clark, and C. H. Liu
977 (2013b) Importance of regional climate model grid spacing for the simulation of heavy
978 precipitation in the Colorado headwaters. *J. Clim.* 26(13):4848–4857.

979

980 Prein, A. F., W. Langhans, G. Fosser, A. Ferrone, N. Ban, K. Goergen, M. Keller, M. Tölle,
981 O. Gutjahr, F. Feser, et al. (2015) A review on regional convection-permitting climate
982 modeling: Demonstrations, prospects, and challenges. *Rev. Geophys.* 53:323–361.

983

984 Rasmussen, R., et al. (2014) Climate change impacts on the water balance of the Colorado
985 headwaters: High-resolution regional climate model simulations. *J. Hydrometeorol.* 15:1091–
986 1116. doi: [10.1175/JHM-D-13-0118.1](https://doi.org/10.1175/JHM-D-13-0118.1).

987

988 Ribes A., Soulihanh T., Vautard R., Dubuisson B., Somot S., Colin J., Planton S.,
989 Soubeyroux J.-M., Observed increase in extreme daily rainfall in the French Mediterranean.
990 *Clim. Dyn.* (*under revision*)

991

992 Siebesma AP, Soares P, Teixeira J. (2007) A combined eddy diffusivity mass-flux approach
993 for the convective boundary layer. *J. Atmos. Sci.* 64:1230–1248.

994

995 Schwitalla, T., H.-S. Bauer, V. Wulfmeyer, and K. Warrach-Sagi (2017) Continuous high-
996 resolution midlatitude-belt simulations for July–August 2013 with WRF. *Geosci. Model Dev.*
997 10:2031-2055. <https://doi.org/10.5194/gmd-10-2031-2017>.

998

999 Scherrer, S. C., M. Begert, M. Croci-Maspoli and C. Appenzeller (2016) Long series of Swiss
1000 seasonal precipitation: regionalization, trends and influence of large-scale flow. *Int. J.*
1001 *Climatol.* (in press) DOI: 10.1002/joc.4584
1002
1003 Shepherd, T.G. (2014). Atmospheric circulation as a source of uncertainty in climate change
1004 projections. *Nature Geoscience* 7(10):703-708.
1005
1006 Sherwood, S.C., Bony, S. and Dufresne, J.L. (2014) Spread in model climate sensitivity
1007 traced to atmospheric convective mixing. *Nature* 505(7481):37-42.
1008
1009 Soares PMM, Miranda PMA, Siebesma AP, Teixeira J. (2004) An eddydiffusivity/mass-flux
1010 parametrization for dry and shallow cumulus convection. *Q. J. R. Meteorol. Soc.* 130: 3365–
1011 3384.
1012
1013 Stéfanon, M., Drobinski, P., D’Andrea, F., Lebeaupin-Brossier, C. and Bastin, S. (2014) Soil
1014 moisture-temperature feedbacks at meso-scale during summer heat waves over Western
1015 Europe. *Climate dynamics*, 42(5-6):1309-1324.
1016
1017 Stevens, B. and Bony, S. (2013) What are climate models missing?. *Science* 340(6136):1053-
1018 1054.
1019
1020 Stucki, P., Brönnimann, S., Martius, O., Welker, C., Rickli, R., Dierer, S., Bresch, D.N.,
1021 Compo, G.P. and Sardeshmukh, P.D. (2015) Dynamical downscaling and loss modeling for
1022 the reconstruction of historical weather extremes and their impacts: a severe Foehn storm in
1023 1925. *Bulletin of the American Meteorological Society* 96(8):1233-1241.

1024

1025 Tabary P, Dupuy P, Lhenaff G, Gueguen C, Moulin L, Laurantin O, Merlier C, Soubeyroux

1026 JM (2012) A 10-year (1997—2006) reanalysis of quantitative precipitation estimation over

1027 France: methodology and first results. *IAHS-AISH* 351:255-260.

1028

1029 Tebaldi, C. and Knutti, R. (2007) The use of the multi-model ensemble in probabilistic

1030 climate projections. *Philosophical Transactions of the Royal Society of London A:*

1031 *Mathematical, Physical and Engineering Sciences* 365(1857):2053-2075.

1032

1033 Teixeira, J., et al. (2008), Parameterization of the atmospheric boundary layer, *Bull. Am.*

1034 *Meteorol. Soc.* 89(4):453–458. doi:10.1175/BAMS- 89-4-453.

1035

1036 Teixeira, J., S. Cardoso, M. Bonazzola, J. Cole, A. Del Genio, C. DeMott, C. Franklin, C.

1037 Hannay, C. Jakob, Y. Jiao, J. Karlsson, H. Kitagawa, M. Köhler, A. Kuwano-Yoshida, C.

1038 LeDrian, J. Li, A. Lock, M.J. Miller, P. Marquet, J. Martins, C.R. Mechoso, E.van Meijgaard,

1039 I. Meinke, P.M.A. Miranda, D. Mironov, R. Neggers, H.L. Pan, D.A. Randall, P.J. Rasch, B.

1040 Rockel, W.B. Rossow, B. Ritter, A.P. Siebesma, P.M.M. Soares, F.J. Turk, P.A. Vaillancourt,

1041 A. Von Engeln, and M. Zhao (2011) Tropical and sub-tropical cloud transitions in weather

1042 and climate prediction models: The GCSS/WGNE Pacific Cross-section Intercomparison

1043 (GPCI). *J. Climate* 24:5223-5256. doi:10.1175/2011JCLI3672.1.

1044

1045 Tölle, M. H., O. Gutjahr, J. Thiele, G. Busch (2014) Increasing bioenergy production on

1046 arable land: Does the regional and local climate respond? Germany as a case study. *Journal of*

1047 *Geophysical Research Atmospheres* 119(6):2711–2724. doi:10.1002/2013JD020877.

1048

1049 Tölle, M. H., L. Schefczyk, O. Gutjahr (2017) Scale dependency of regional climate
1050 modeling of current and future climate extremes in Germany. Theoretical and Applied
1051 Climatology. DOI: 10.1007/s00704-017-2303-6
1052

1053 Vautard, R., G.-J. van Oldenborgh, S. Thao, B. Dubuisson, G. Lenderink, A. Ribes, S.
1054 Planton, J.-M. Soubeyroux, P. Yiou (2015) Extreme fall precipitations in the Cévennes
1055 mountains. Bull. Am. Meteorol. Soc. Suppl. On “explaining extreme events of 2014 from a
1056 climate perspective” 96:S56-S60.
1057

1058 Warrach-Sagi, K., T. Schwitalla, V. Wulfmeyer, and H.-S. Bauer (2013) Evaluation of a
1059 Climate Simulation in Europe Based on the WRF-NOAH Model System: Precipitation in
1060 Germany. Climate Dynamics 41:755-774.
1061

1062 Wu, L. (2009), Comparison of atmospheric infrared sounder temperature and relative
1063 humidity profiles with NASA African Monsoon Multidisciplinary Analyses (NAMMA)
1064 dropsonde observations, J. Geophys. Res. 114, D19205, doi:10.1029/2009JD012083.
1065

1066 Mark J. Webb, Adrian P. Lock, Christopher S. Bretherton, Sandrine Bony, Jason N. S. Cole,
1067 Abderrahmane Idelkadi, Sarah M. Kang, Tsuyoshi Koshiro, Hideaki Kawai, Tomoo Ogura,
1068 Romain Roehrig, Yechul Shin, Thorsten Mauritsen, Steven C. Sherwood, Jessica Vial,
1069 Masahiro Watanabe, Matthew D. Woelfle, Ming Zhao, (2015) The impact of parametrized
1070 convection on cloud feedback. Philos. Tran. of the Royal Soc. A,
1071 DOI:10.1098/rsta.2014.0414
1072
1073

1074 Weisman, M. L., W. Skamarock, and J. B. Klemp (1997) The resolution dependence of
1075 explicitly modeled convective systems. *Monthly Weather Review* 125:527-548,
1076 doi:10.1175/1520-0493(1997)125<0527:TRDOEM>[2.0.CO;2](#).
1077

1078 Westra, S., H. J. Fowler, J. P. Evans, L. V. Alexander, P. Berg, F. Johnson, E. J. Kendon, G.
1079 Lenderink, and N. M. Roberts (2014) Future changes to the intensity and frequency of short-
1080 duration extreme rainfall. *Rev. Geophys.* 52:522–555. doi:10.1002/2014RG000464.
1081

1082 Wüest, M., Frei, C., Altenhoff, A., Hagen, M., Litschi, M. and Schär, C. (2010) A gridded
1083 hourly precipitation dataset for Switzerland using rain-gauge analysis and radar-based
1084 disaggregation. *Int. J. Climatol.* 30:1764–1775. doi:10.1002/joc.2025
1085

1086 Yano, J.I., Soares, P.M.M., Köhler, M. and Deluca, A. (2015) The Convective
1087 Parameterization Problem: Breadth and Depth. *Bulletin of the American Meteorological*
1088 *Society* 96(8):ES127-ES130.
1089

1090 Yano, J.I., Ziemiański, M.Z., Cullen, M., Termonia, P., Onvlee, J., Bengtsson, L., Carrassi,
1091 A., Davy, R., Deluca, A., Gray, S.L. and Homar, V., (2017) Scientific challenges of
1092 convective-scale numerical weather prediction. *Bulletin of the American Meteorological*
1093 *Society*.
1094

1095 Zappa, G., & Shepherd, T. G. (2017). Storylines of atmospheric circulation change for
1096 European regional climate impact assessment. *Journal of Climate*, 30(16), 6561-6577.

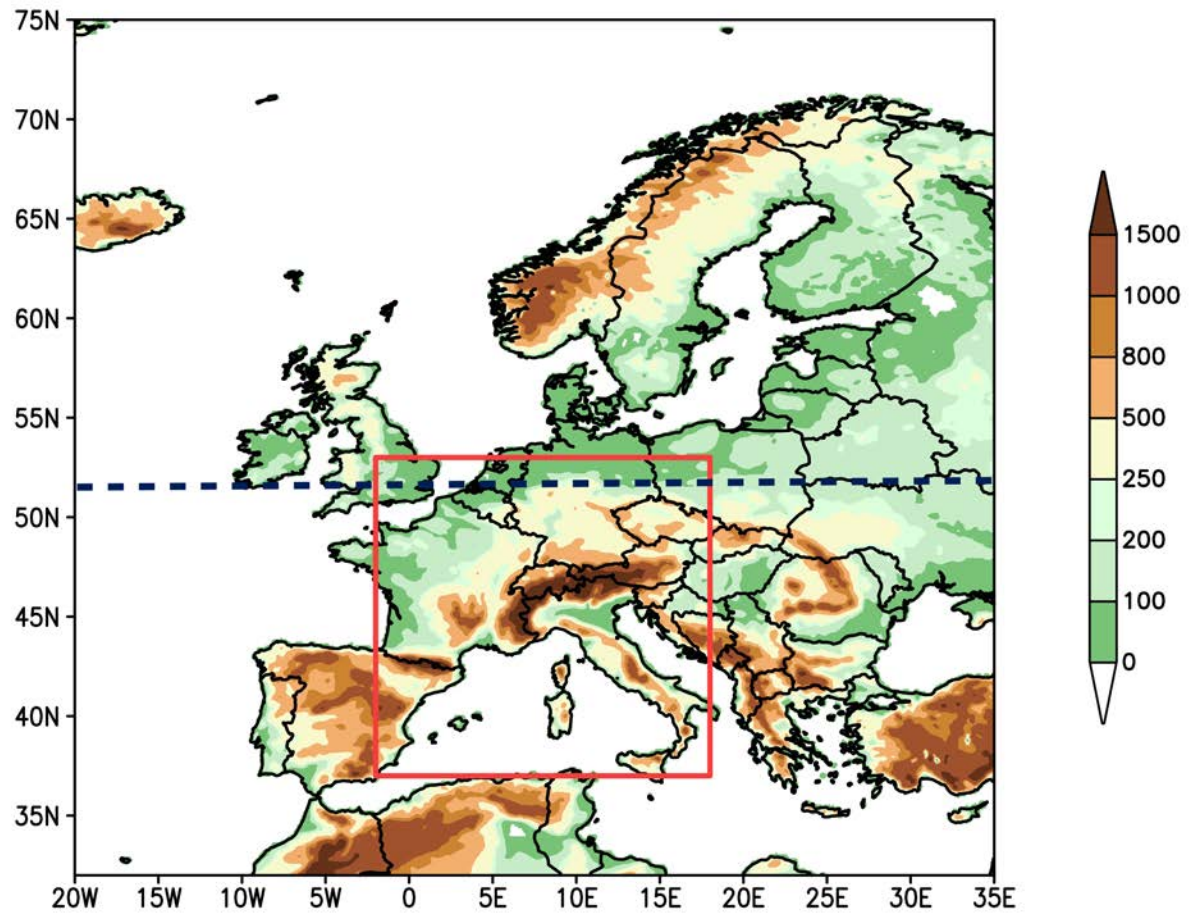
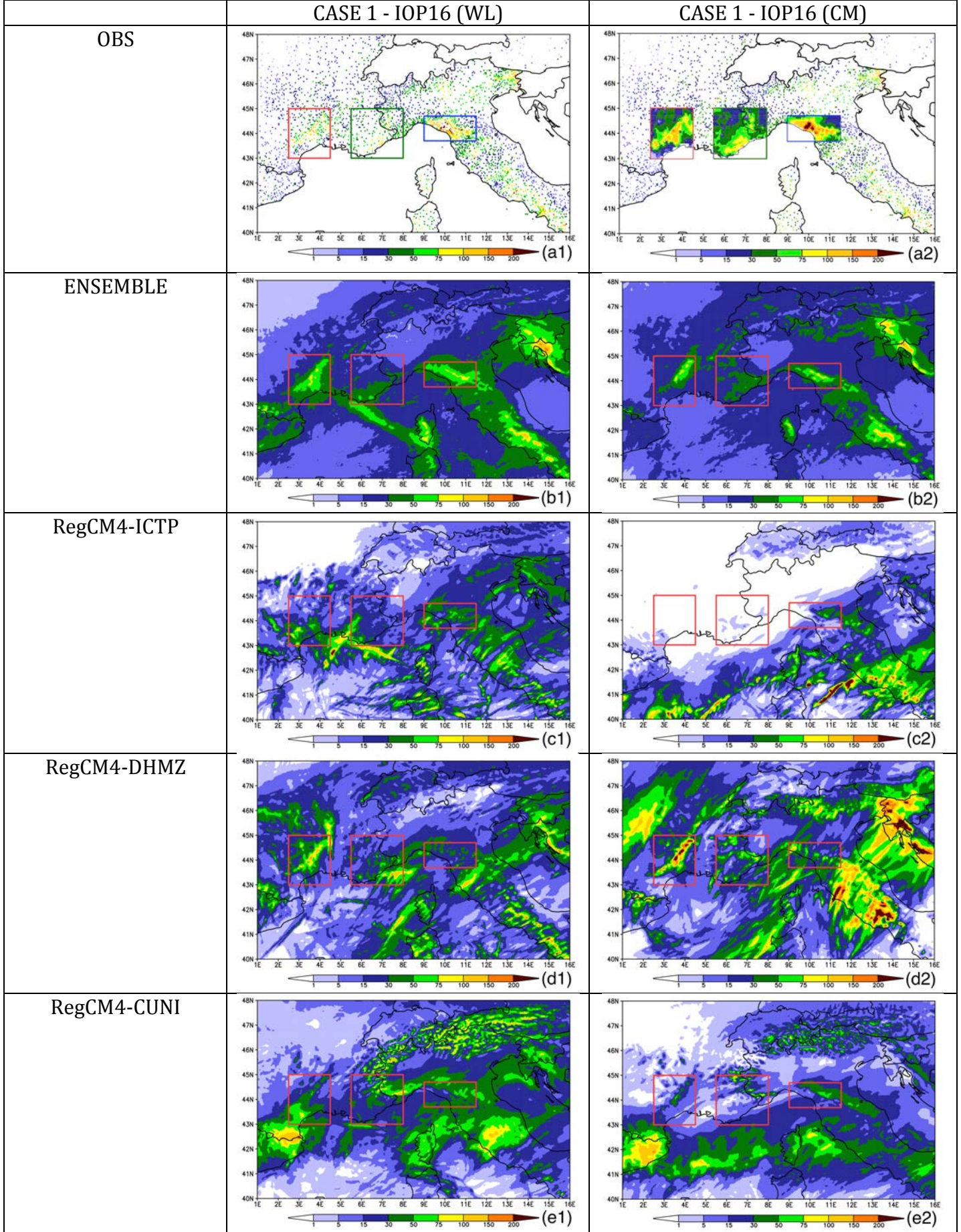
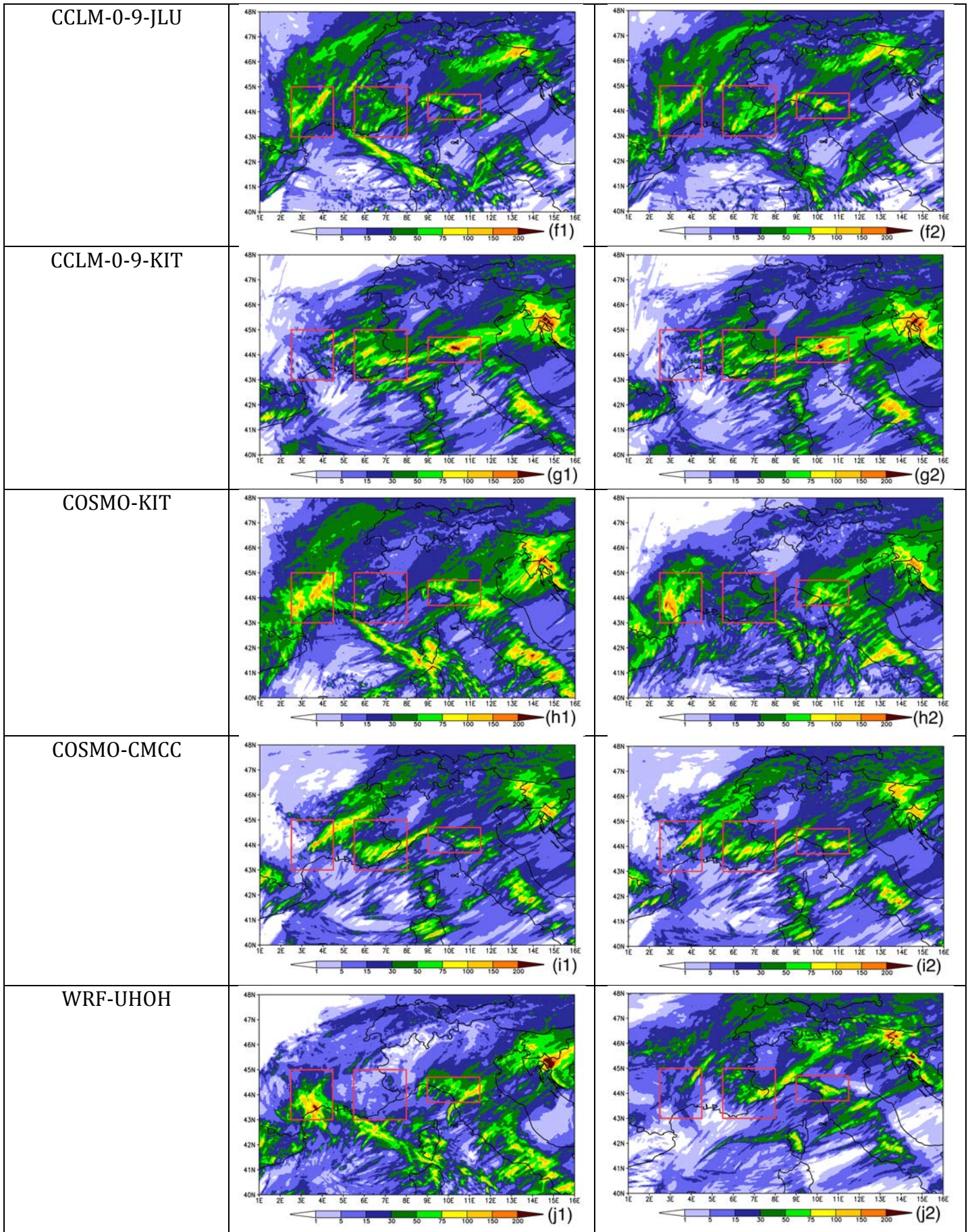


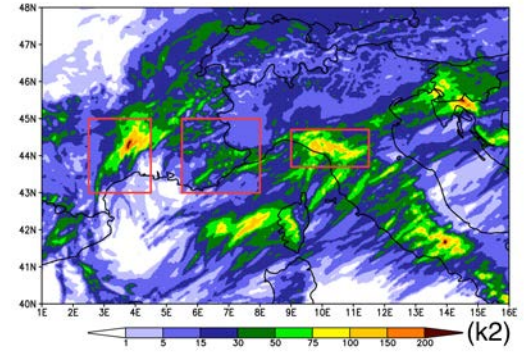
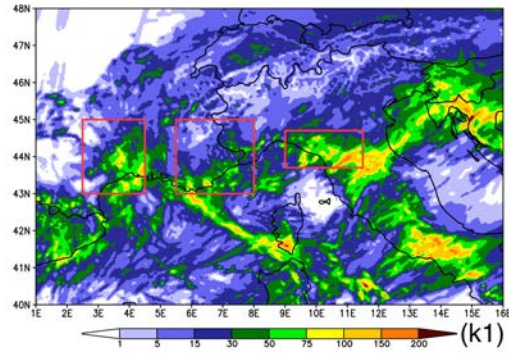
Figure 1: Euro-CORDEX domain at 0.11 degrees resolution with highlighted red box for FPS mandatory domain. The blue dashed line represents the Northern boundary of the Med-CORDEX domain.

Total accumulated precipitation during the event (mm)

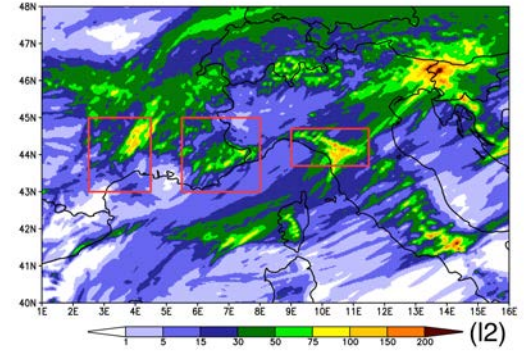
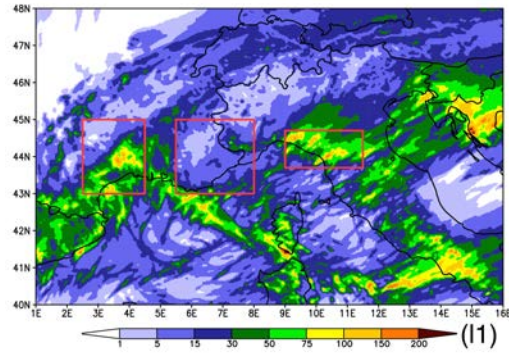




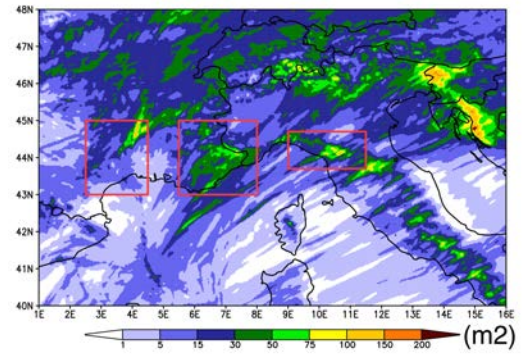
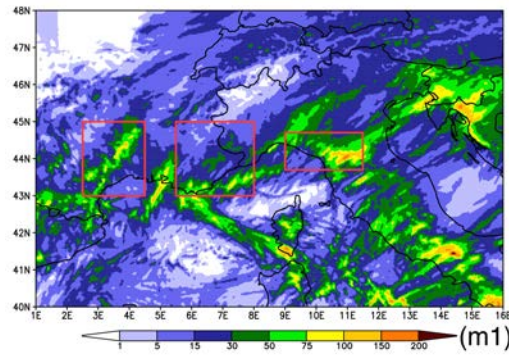
WRF-AUTH-MC



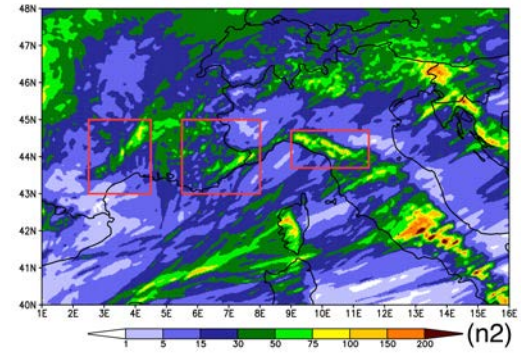
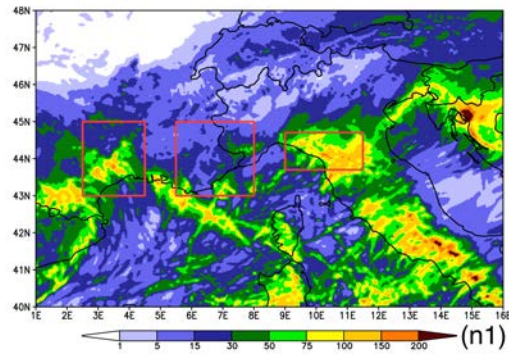
WRF-FZJ-IBG3



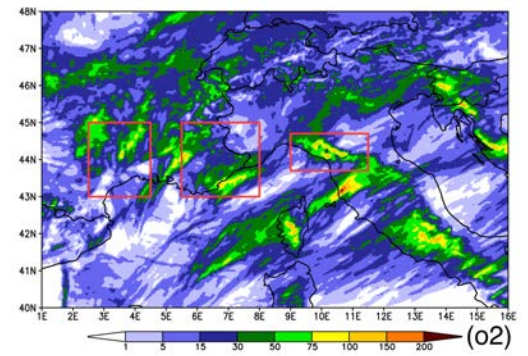
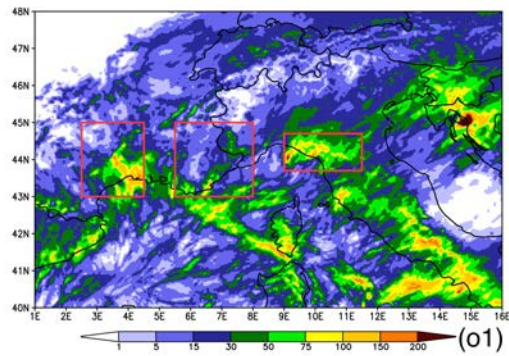
WRF-IPSL

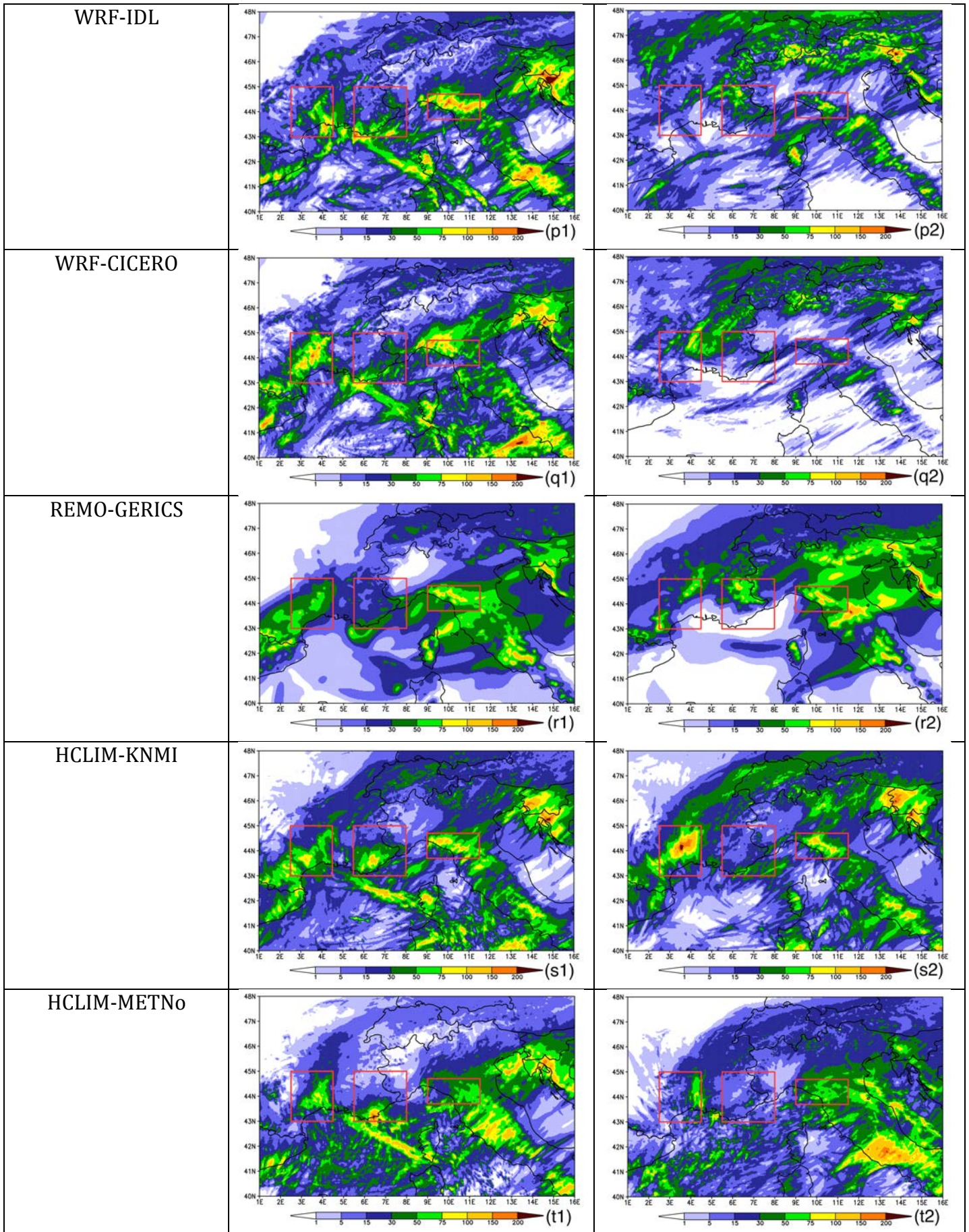


WRF-BCCR



WRF-UNICAN





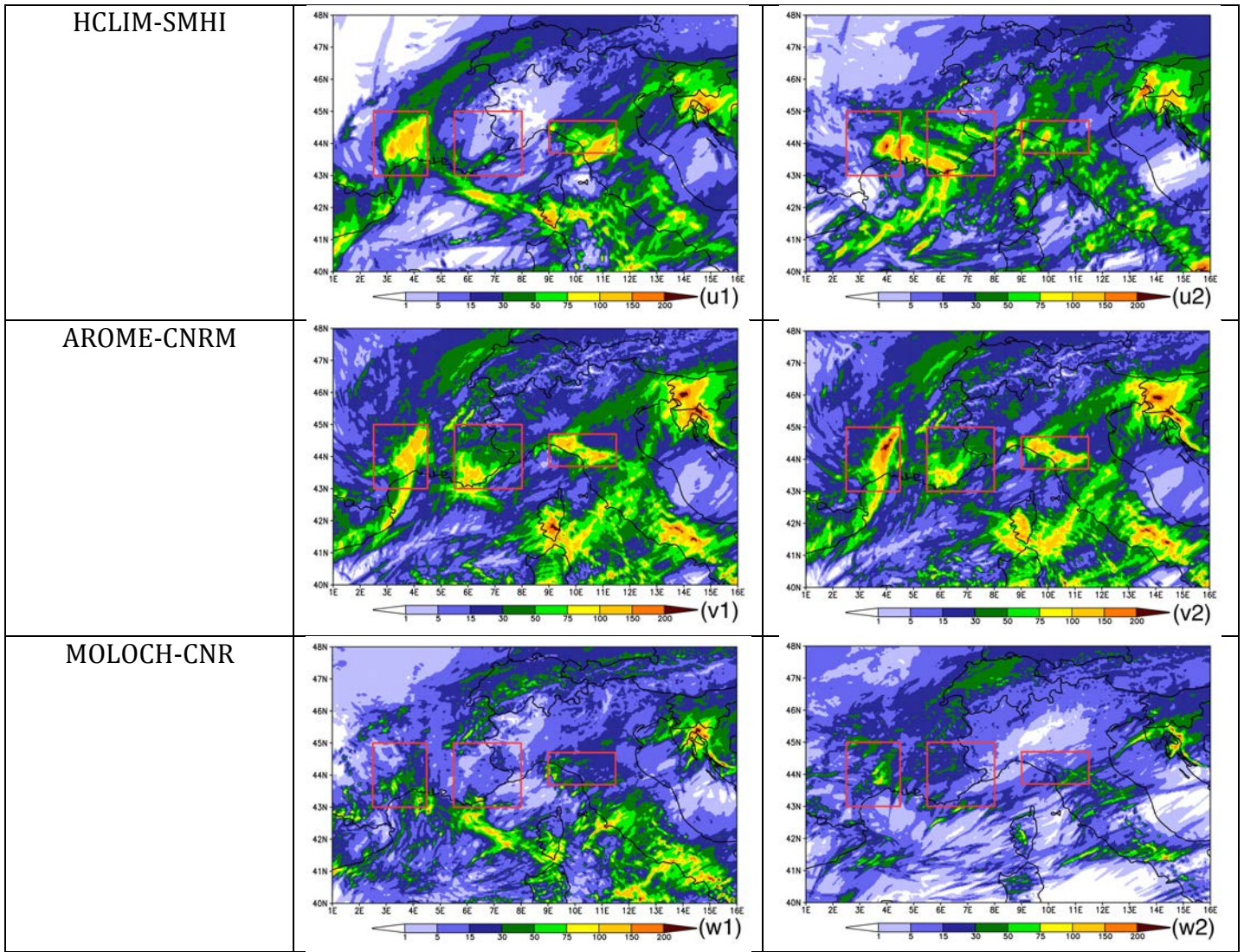


Figure 2: CASE 1 - HyMeX-IOP16. Total accumulated precipitation (mm) for observations, multi-model ensemble mean (MEM) and each ensemble member. Results are shown for the models run in WL mode (left) and in CM (right). Red, green and blue boxes on panels (a1) and (a2) indicate specific areas of interest. Panel (a2) shows an interpolation of the observed precipitation field.

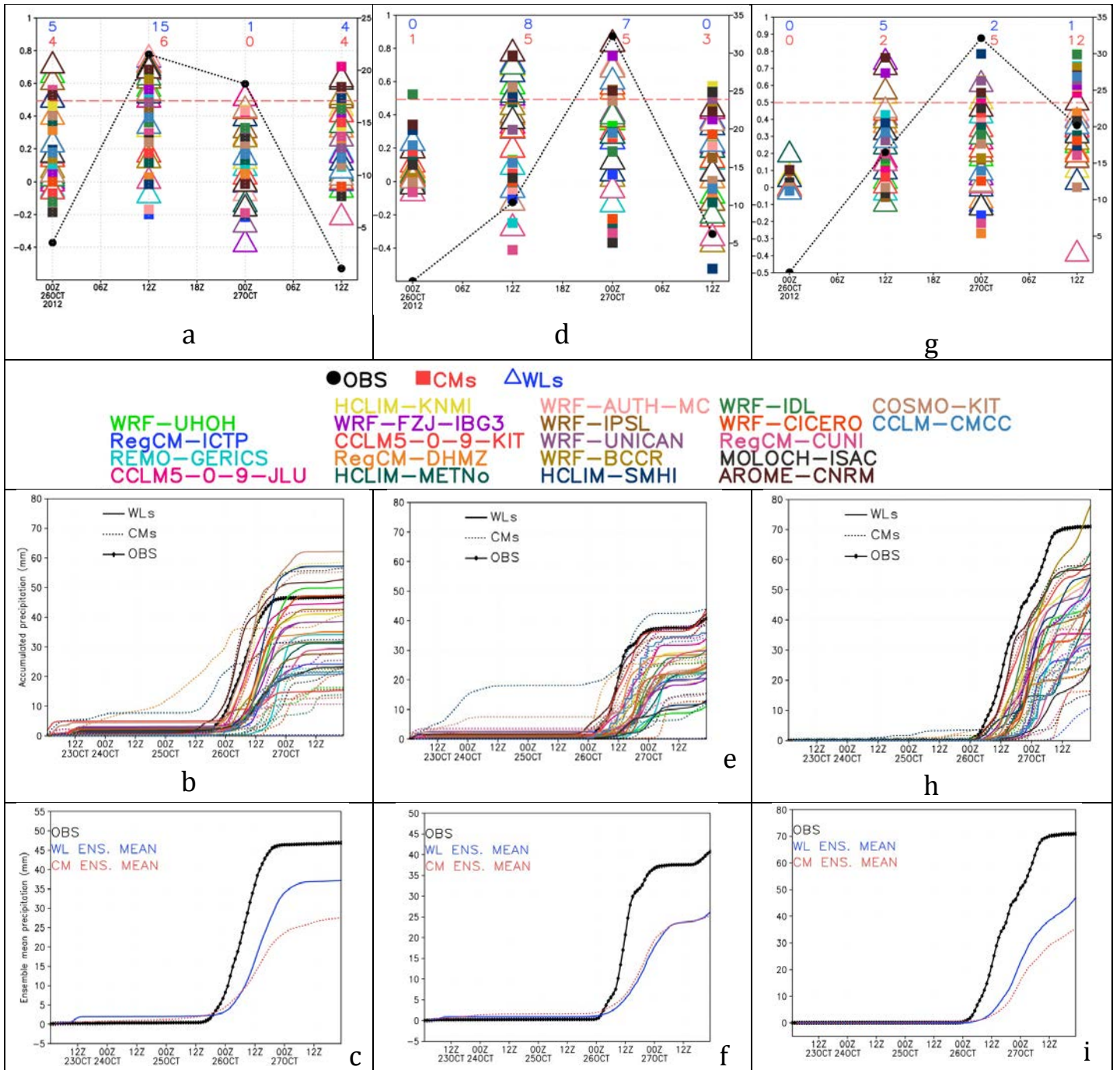
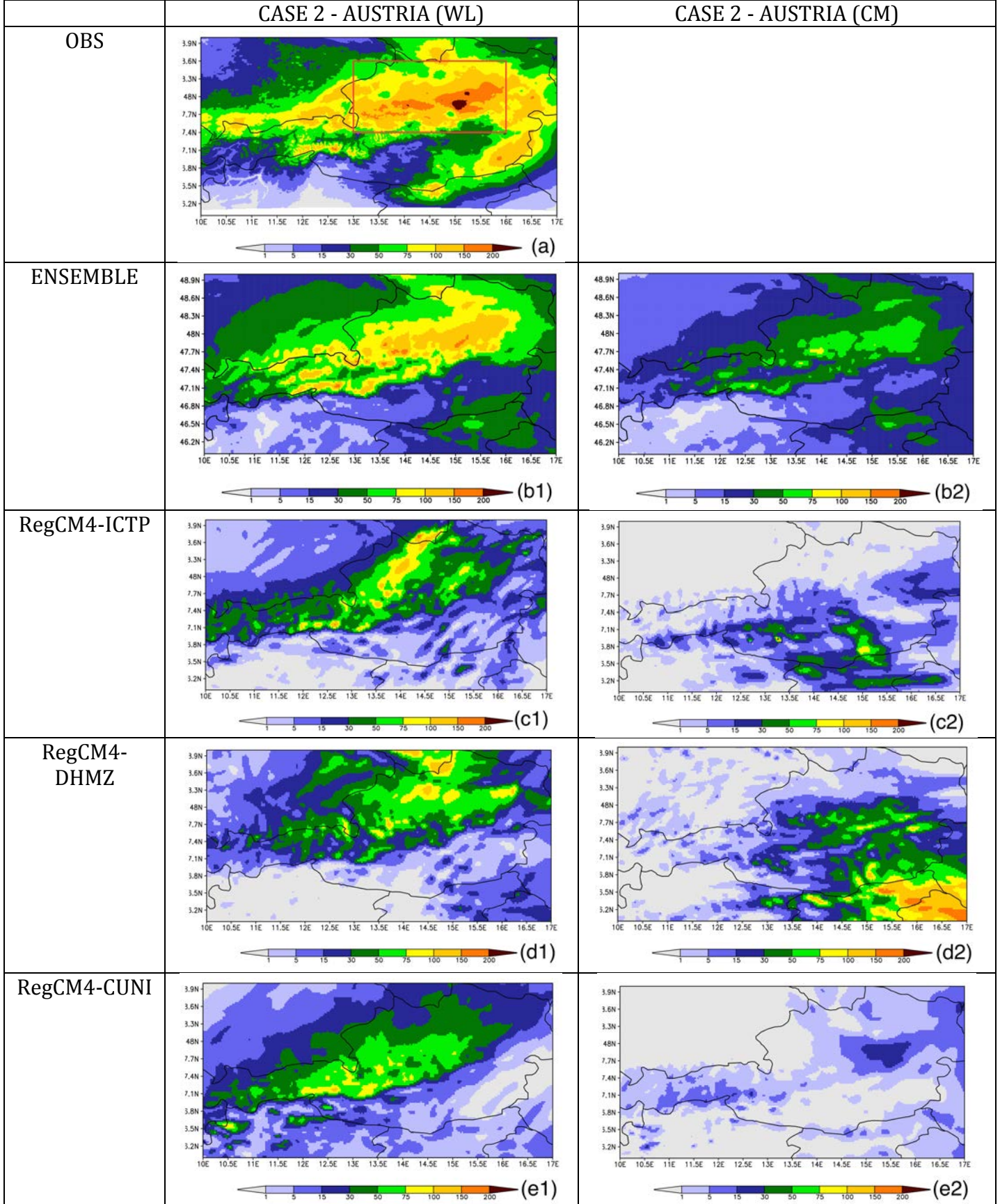
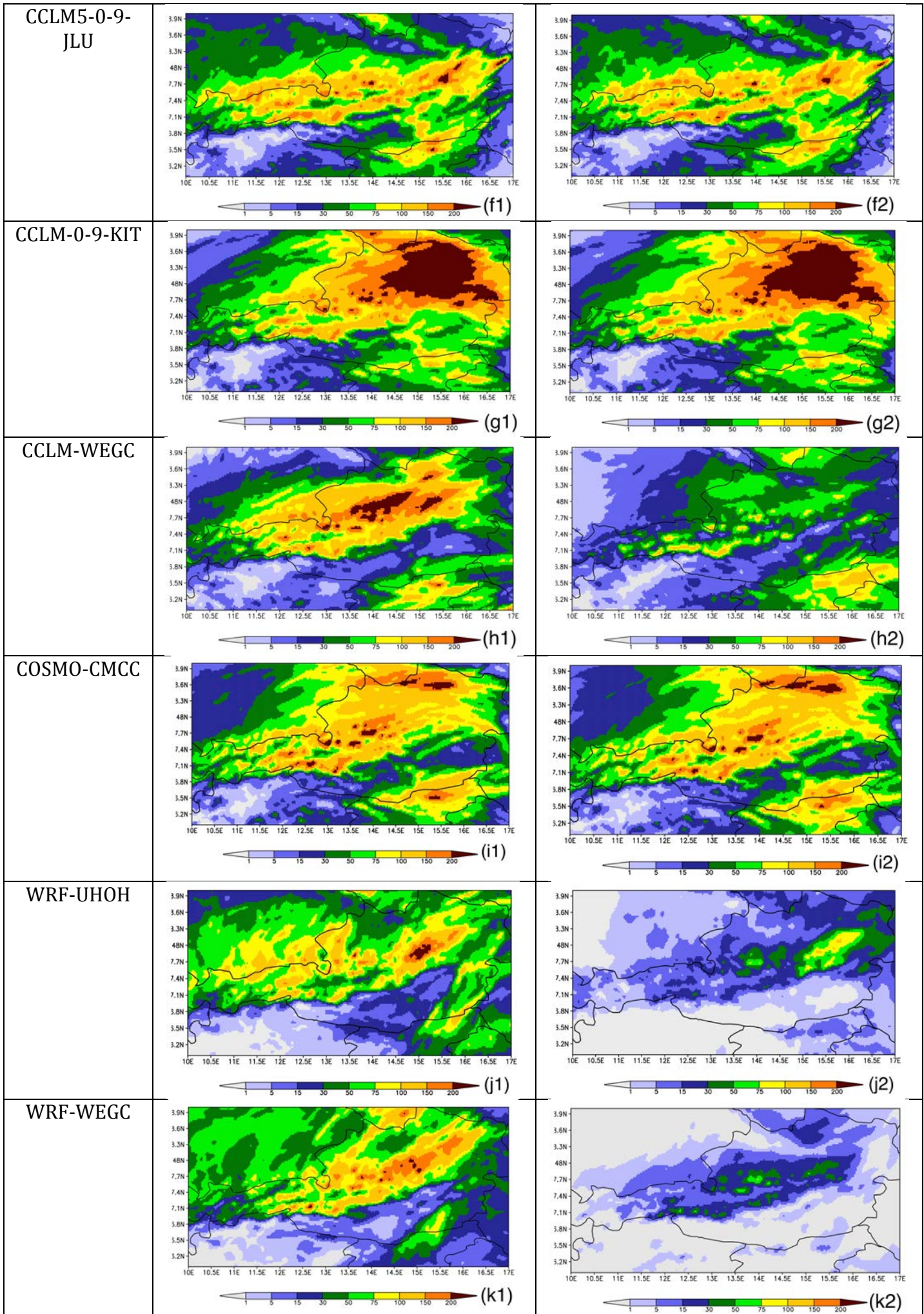
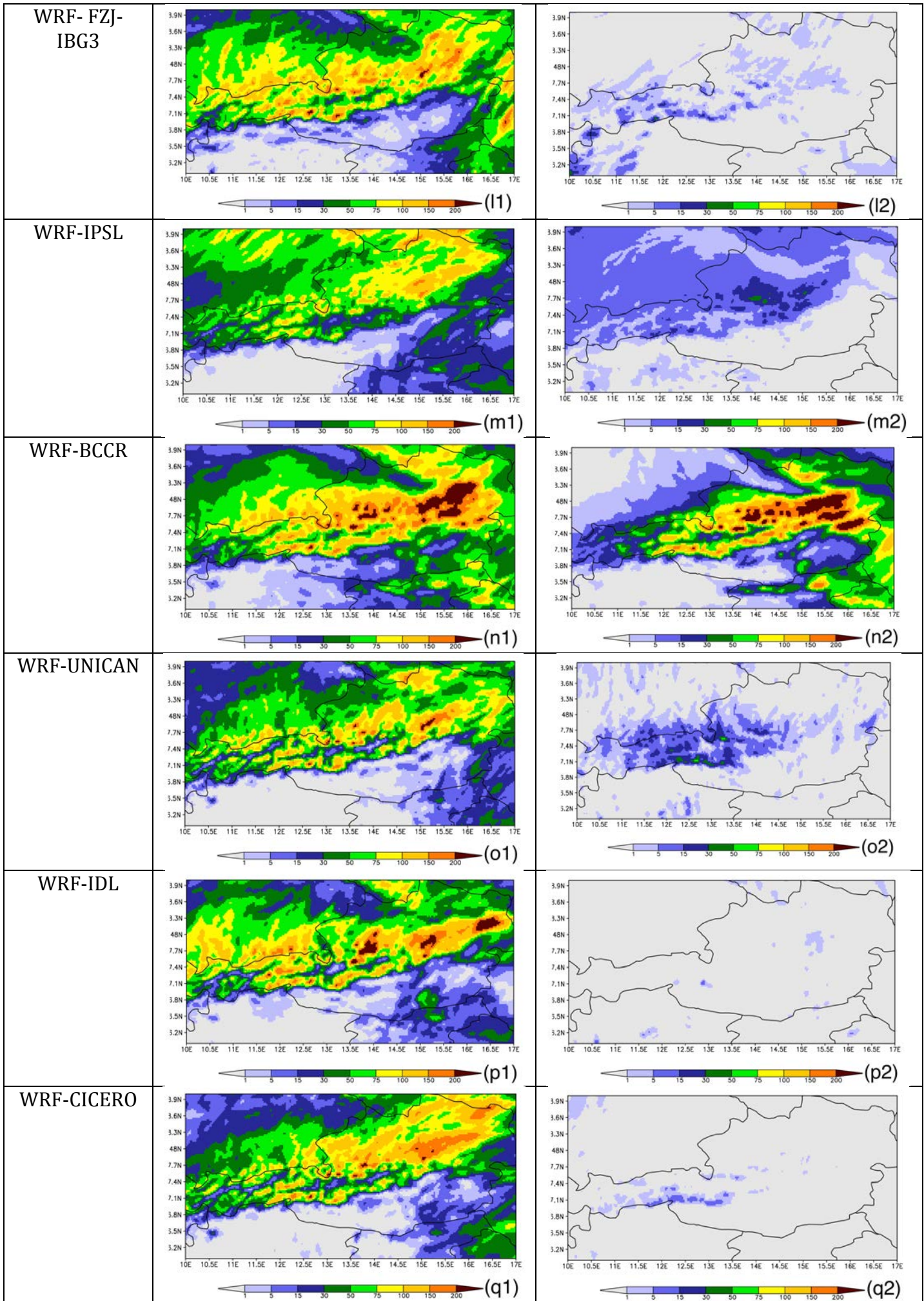


Figure 3: Time series of the 12 hours accumulated precipitation (in mm on the y-axis) during the event and temporal evolution of the spatial correlation between simulations and interpolated observation of the 12 hours accumulated precipitation, over CV1, CV2 and LT boxes (panels (a,d,g)). Left hand side y-axes refer to correlation (colored symbols); right hand side y-axes refer to the accumulated precipitation (black line). Numbers of models with a correlation greater than 0.5 for WL simulation (in blue) and CM simulation (in red) are reported on the top of each plots. Time series of the hourly accumulated precipitation averaged over the red, green and blue boxes (Fig. 1a) for each model and observations (panels b,e and h). Time series of hourly accumulated precipitation ensemble mean (WL and CM respectively in blue and red) and observations (black) for the three areas of interest (panels c,f and i).

Total accumulated precipitation during the event (mm)







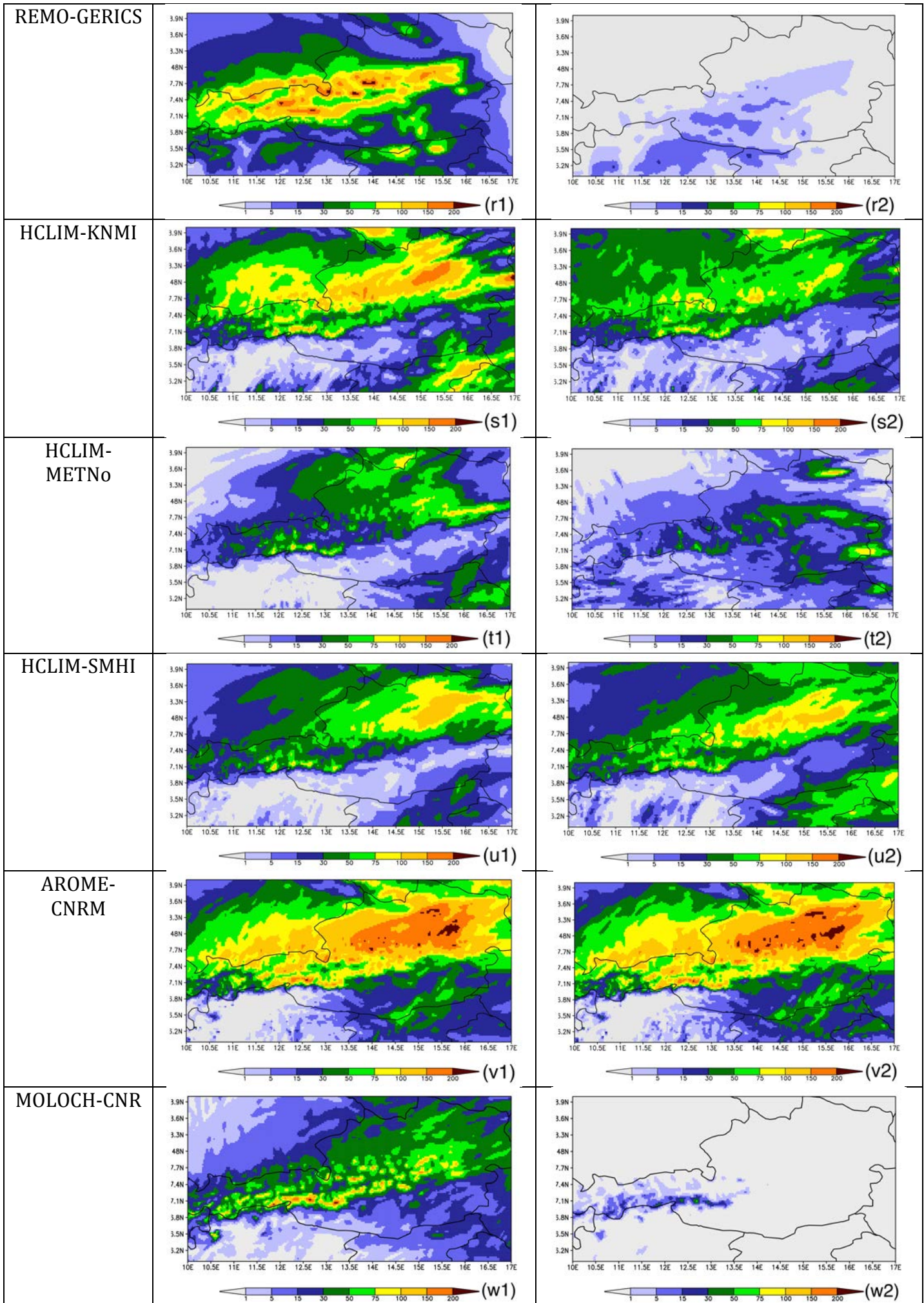


Figure 4: CASE 2 - AUSTRIA. Total accumulated precipitation (mm) for observations, multi-model ensemble mean and each ensemble member. Results are shown for the models run in WL mode (left) and in CM (right). Red box on panel (a) indicates specific area of interest.

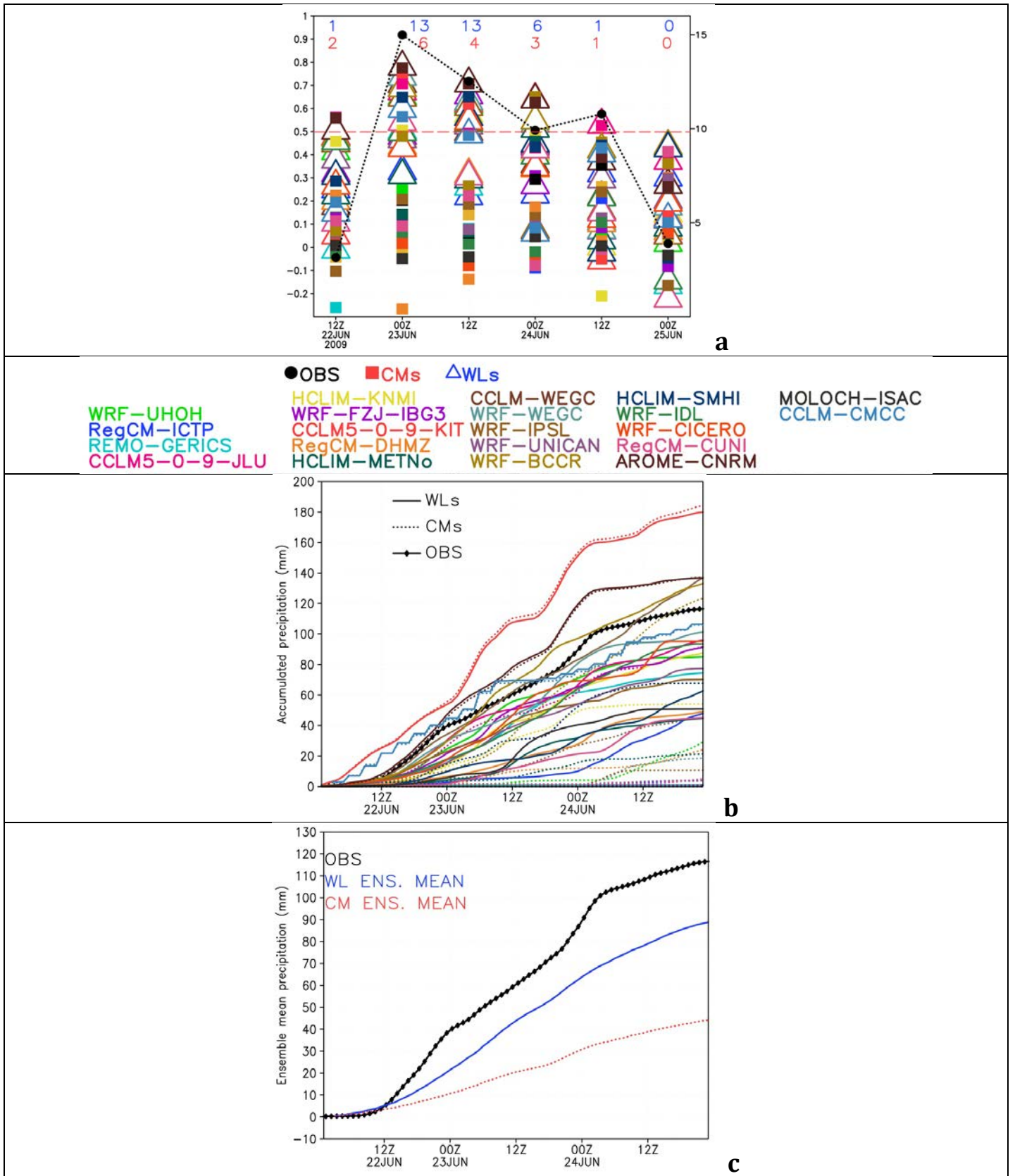
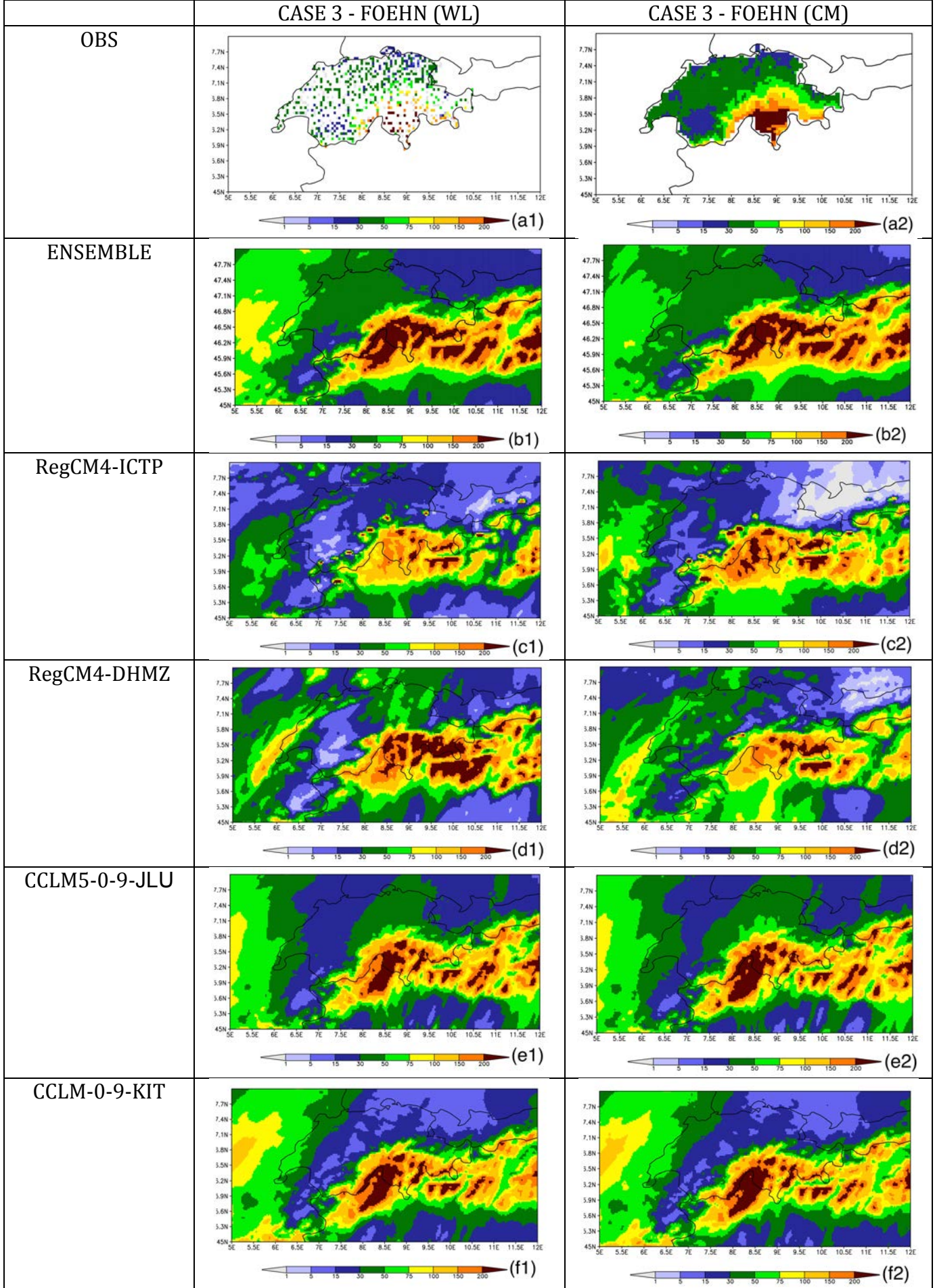
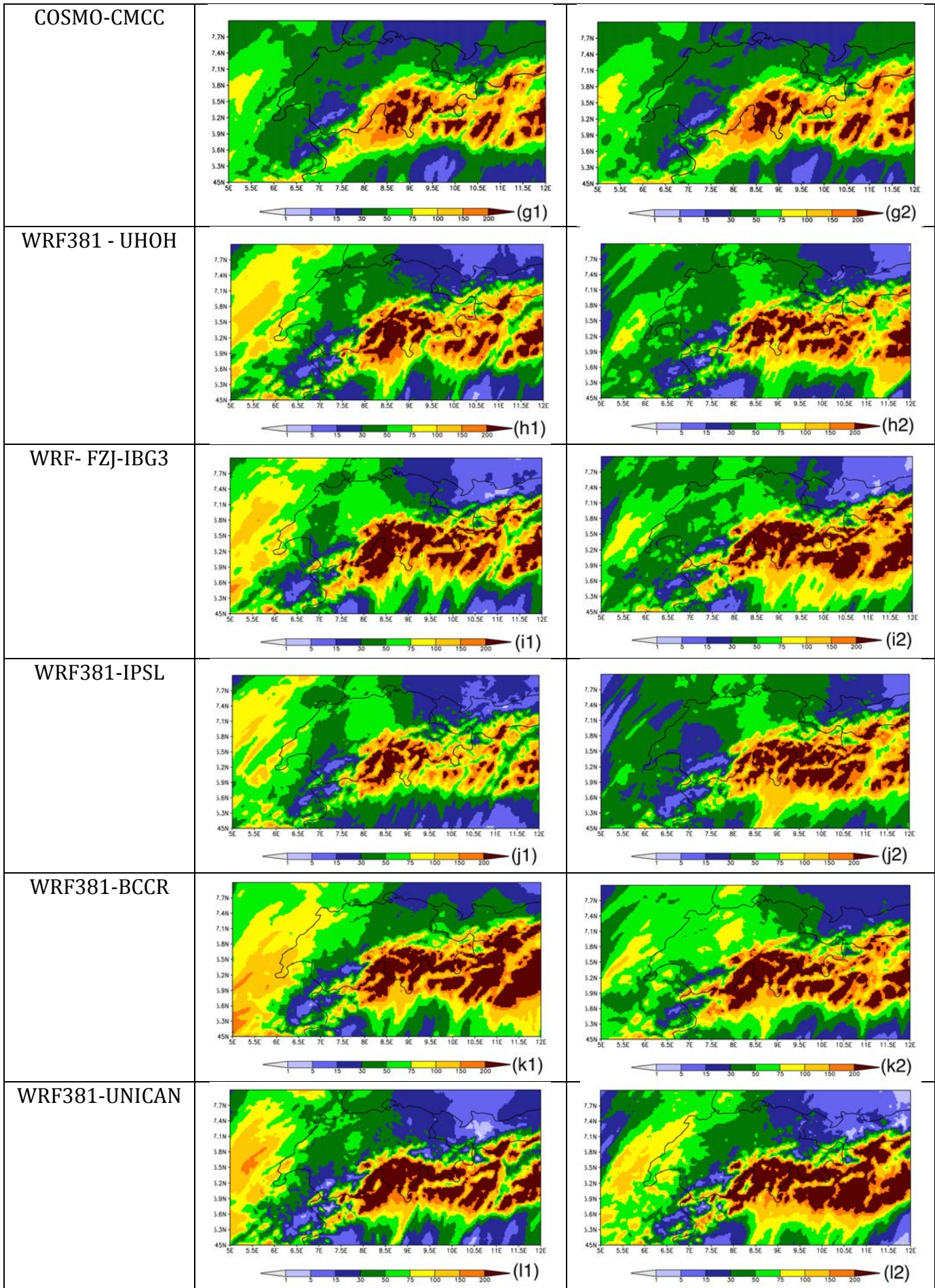
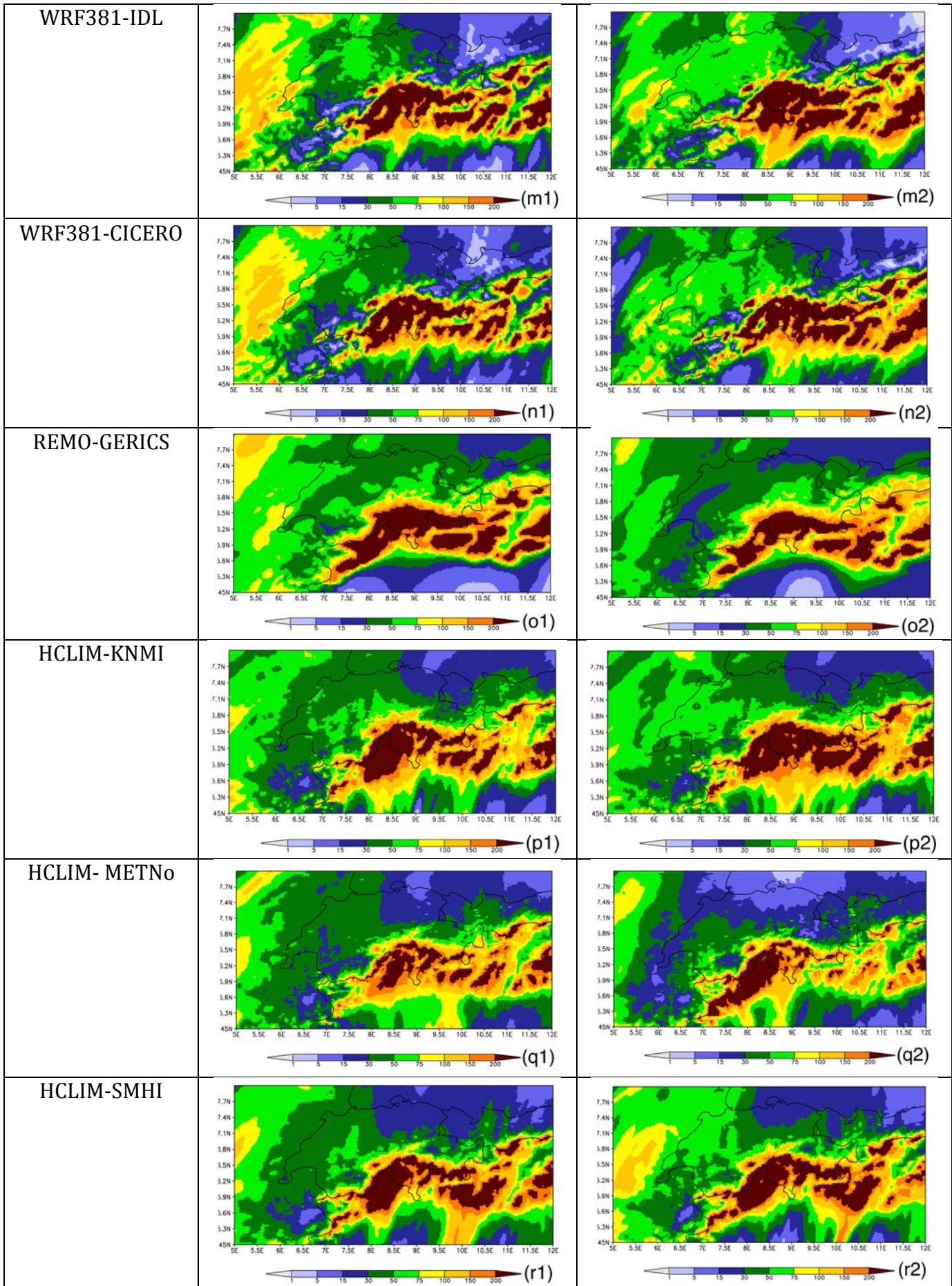


Figure 5: Time series of the 12 hours accumulated precipitation (in mm on the y-axis) during the event and temporal evolution of the spatial correlation of the accumulated 12 hours precipitation between the simulations and observation (panel a). Left hand side y-axes refer to correlation (colored symbols); right hand side y-axes refer to the accumulated precipitation (black line). Numbers of models with a correlation greater than 0.5 for WL simulation (in blue) and CM simulation (in red). Time series of the precipitation averaged over the red area (Fig. 3a) for each model and observations (panel b). Time series of hourly accumulated precipitation ensemble mean (WL and CM respectively in blue and red) and observations (black) over the area of interest (panel c).

Total accumulated precipitation during the event (mm)







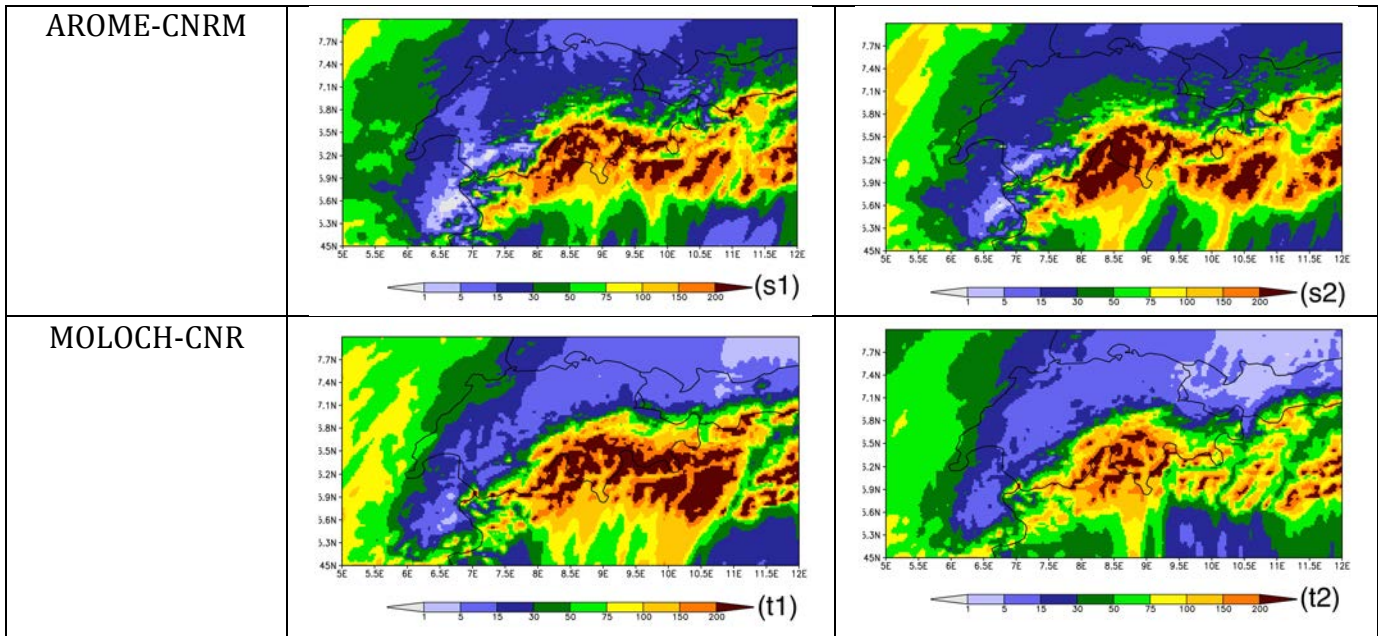


Figure 6: CASE 3 - FOEHN. Total accumulated precipitation (mm) for observations, multi-model ensemble mean and each ensemble member. Results are shown for the models run in WL mode (left) and in CM (right). Panel (a2) shows an interpolation of the observed precipitation field.

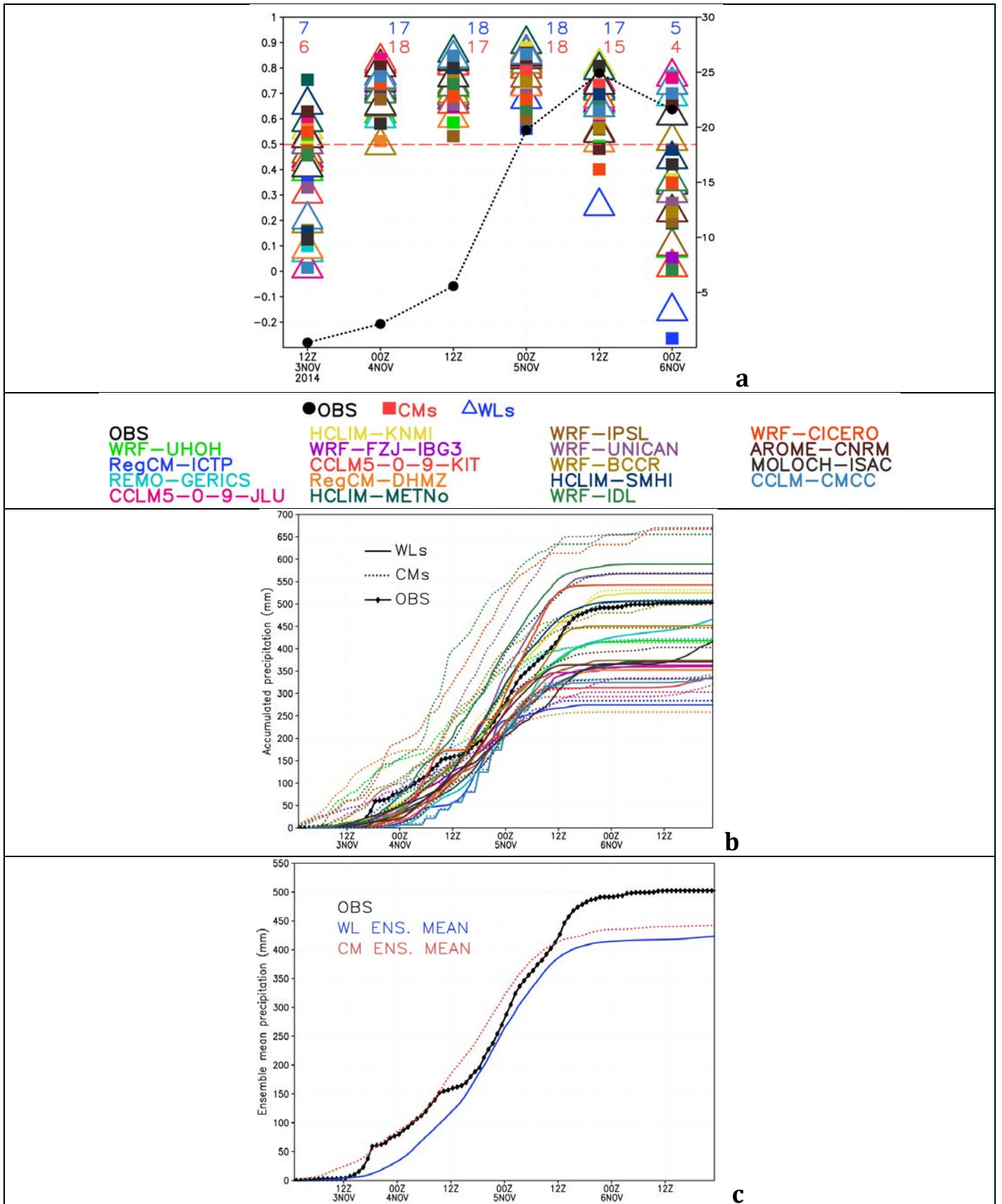


Figure 7: Time series of the 12 hours accumulated precipitation (in mm on the y-axis) during the event and temporal evolution of the spatial correlation of the accumulated 12 hours precipitation between the simulations and observation (panel a). Left hand side y-axes refer to correlation (colored symbols); right hand side y-axes refer to the accumulated precipitation (black line). Numbers of models with a correlation greater than 0.5 for WL simulation (in blue) and CM simulation (in red). Time series of the precipitation averaged over the region covered by the observations (Fig. 6a) for each model and observations (panel b). Time series of hourly accumulated precipitation ensemble mean(WL and CM respectively in blue and red) and observations (black) over the observation area (panel c).

Table 1: List of contributors.

	Contributor's ID	Contact Person	Model	Institute	Testcases	Climate Scenario Simulation	Nudging (Yes/No)	Resolution of the feeding domain
1	RegCM4-ICTP	Erika Coppola	RegCM4	Abdus Salam International Centre for Theoretical Physics - Earth System Physics	√	√	No	0.11 EURO-CORDEX
2	RegCM4-DHMZ	Ivan Guettler	RegCM4	Meteorological and Hydrological Service of Croatia	√	√	No	0.11 EURO-CORDEX
3	RegCM4-CUNI	Michal Belda	RegCM4	Univerzita Karlova, Matematicko-fyzikální fakulta, Praha	√	√	No	
4	CCLM-JLU	Merja Toelle	CCLM5-0-9	Justus-Liebig University of Giessen, Department of Geography, Climatology, Climate Dynamics and Climate Change	√	√	No	0.75 ERAINT
5	CCLM-KIT	Hans-Juergen Panitz	CCLM5-0-9	Karlsruhe Institute of Technology	√	√	No	0.22 EURO-CORDEX
6	CCLM-WEGC	Marie Piazza	CCLM5-0-9	Wegener Center for Climate and Global Change, University of Graz	√	√	No	0.11 EURO-CORDEX
7	COSMO-KIT	Samiro Khodayar	CCLM5-0-9	Karlsruhe Institute of Technology	√		No	0.11 EURO-CORDEX
8	COSMO-CMCC	Mario Raffa	CCLM5-0-9	Euro-Mediterranean Center on Climate Change	√	√	No	0.22 EURO-CORDEX
9	CCLM-GUF	Bodo Ahrens	CCLM	Goethe University Frankfurt am Main		√	No	0.11 EURO-CORDEX
10	CCLM-ETH	Nikolina Ban	CCLM	Institut für Atmosphäre und Klima, ETH Zürich		√	No	
11	WRF-UHOH	Josipa Milovac	WRF	University of Hohenheim, Germany	√	√	No	0.11 EURO-CORDEX

12	WRF-WEGC	Heimo Truhetz	WRF	Wegener Center for Climate and Global Change, University of Graz	√	√	No	0.11 (WL) 15km (CM)
13	WRF-AUTH-MC	Eleni Katragkou	WRF	Aristotle University of Thessaloniki, Department of Meteorology & Climatology	√	√	No	0.11 EURO-CORDEX
14	WRF-FZJ-IBG3	Klaus Goergen	WRF	Research Centre Jülich, Institute of Bio- and Geosciences (Agrosphere, IBG-3)	√	√	No	0.11 EURO-CORDEX
15	WRF-IPSL	Lluís Fita Borrell	WRF	The Institute Pierre Simon Laplace, Paris	√	√	No	0.11 EURO-CORDEX
16	WRF-BCCR	Stefan Sobolowski	WRF	Bjerknes Centre for Climate Research	√	√	No	0.11 EURO-CORDEX
17	WRF-UNICAN	Jesus Fernandez	WRF	Santander Meteorology Group, Universidad de Cantabria, Dept. Applied Mathematics and Comp. Sci.	√	√	No	0.11 EURO-CORDEX
18	WRF-IDL	Rita Margarida Cardoso	WRF	Instituto Dom Luiz, Faculdade de Ciências da Universidade de Lisboa	√	√	No	0.11 EURO-CORDEX
19	WRF-CICERO	Louis Marelle	WRF	Center for International Climate and Environmental Research - Oslo	√	√	No	0.11 EURO-CORDEX
20	WRF-L-IPSL	Robert Vautard	WRF	The Institute Pierre Simon Laplace, Paris		√	No	0.11 EURO-CORDEX
21	WRF-GIUB	Andrey Martynov	WRF	Institute of Geography and Oeschger Centre University of Bern Bern, Switzerland		√	No	
22	REMO-GERICS	Kevin Sieck	REMO2017	Climate Service Center	√	√	No	0.11 EURO-CORDEX

				Germany				
23	HCLIM-KNMI	Hylke de Vries	HCLIM38-AROME	The Royal Netherlands Meteorological Institute	√	√	No	0.11 EURO-CORDEX
24	HCLIM-METNo	Andreas Dobler	HCLIM38-AROME	The Norwegian Meteorological Institute	√	√	No	0.11 EURO-CORDEX
25	HCLIM-SMHI	Danijel Belusic	HCLIM38-AROME	Swedish Meteorological and Hydrological Institute	√	√	No	0.11 EURO-CORDEX
26	AROME-CNRM	Samuel Somot	AROME41t1	CNRM-MeteoFrance	√	√	No	0.11 EURO-CORDEX
27	MOLOCH-CNR	Silvio Davolio	MOLOCH	Institute of Atmospheric Sciences and Climate, ISAC-CNR	√		No	0.11 EURO-CORDEX
28	UM10.1-MOHC	Lizzie Kendon	UM10.1	Met Office Hadley Centre		√	No	

Table 2: List of acronyms of the three test cases and initialization procedure.

CASE	ACRONYM	Initialization Procedure	Analyzed Time Window
1	HymexIOP16	Starting DATE (WL): 2012-10-23 Ending DATE (WL): 2012-10-28 Starting DATE (CM): 2012-10-01 Ending DATE(CM): 2012-11-01	23 Oct 2012 00:00 - 28 Oct 2012 00:00
2	AUSTRIA	Starting DATE (WL): 2009-06-20 Ending DATE (WL): 2009-06-27 Starting DATE (CM): 2009-06-01 Ending DATE(CM): 2009-07-01	22 Jun 2009 00:00 - 25 Jun 2009 00:00
3	FOEHN	Starting DATE (WL): 2014-11-02 Ending DATE (WL): 2014-11-07 Starting DATE (CM): 2014-10-01 Ending DATE(CM): 2014-11-07	3 Nov 2014 00:00 - 7 Nov 2014 00:00

Table 3: Spatial correlation of the total accumulated precipitation between simulations and interpolated observation for each of the boxes identified in the Case 1.

Models	CASE 1 - IOP16 Red box (WL)	CASE 1 - IOP16 Red box (CM)	CASE 1 - IOP16 Green box (WL)	CASE 1 - IOP16 Green box (CM)	CASE 1 - IOP16 Blue box (WL)	CASE 1 - IOP16 Blue box (CM)
ENSEMBLE	0.74	0.65	0.67	0.45	0.60	0.77
RegCM4-ICTP	0.30	-0.11	0.20	0.28	-0.02	-0.19
RegCM4-DHMZ	0.62	0.64	0.43	0.15	-0.05	0.22
RegCM4-CUNI	0.07	0.53	-0.03	-0.14	-0.53	-0.24
CCLM-JLU	0.50	0.50	0.41	0.52	0.48	0.57
CCLM-KIT	0.29	0.22	0.24	0.28	0.27	0.36
WRF-UHOH	0.38	0.23	0.35	0.11	0.20	0.61
WRF-AUTH- MC	0.57	0.48	0.58	0.33	0.31	0.75
WRF-FZJ-IBG3	0.44	0.37	0.49	0.50	0.32	0.71
WRF-IPSL	0.56	0.15	0.45	0.38	0.18	0.45
WRF-BCCR	0.50	0.54	0.21	0.24	0.34	0.68
WRF-UNICAN	0.45	0.15	0.49	0.23	0.66	0.68
WRF-IDL	0.52	0.29	0.52	-0.14	0.46	0.60
WRF-CICERO	0.61	0.15	0.51	-0.06	0.27	0.52
REMO-GERICS	0.54	0.06	0.37	-0.36	0.50	0.64
HCLIM-KNMI	0.33	0.64	0.65	0.39	0.54	0.75
HCLIM-METNo	0.56	0.26	0.51	0.45	-0.25	0.29
HCLIM-SMHI	0.66	0.18	0.51	0.37	0.25	0.69
AROME-CNRM	0.71	0.58	0.49	0.56	0.65	0.71
MOLOCH-CNR	0.44	0.48	0.23	-0.20	0.09	0.17
COSMO-KIT	0.57	0.38	0.33	0.49	0.30	0.45
COSMO-CMCC	0.51	0.50	0.54	0.39	0.18	0.33

Table 4: Same as Table 3 but for the Case 2.

Models	CASE 2 -AUSTRIA (WL)	CASE 2 - AUSTRIA (CM)
ENSEMBLE	0.82	0.81
RegCM4-ICTP	0.62	-0.01
RegCM4-DHMZ	0.63	0.02
RegCM4-CUNI	0.49	0.37
CCLM-JLU	0.63	0.62
CCLM-KIT	0.77	0.77
CCLM-WEGC	0.75	0.39
WRF-UHOH	0.69	0.60
WRF-WEGC	0.68	0.61
WRF-FZJ-IBG3	0.62	0.05
WRF-IPSL	0.54	0.47
WRF-BCCR	0.77	0.64
WRF-UNICAN	0.69	0.27
WRF-IDL	0.64	0.10
WRF-CICERO	0.67	0.05
REMO-GERICS	0.44	0.23
HCLIM-KNMI	0.67	0.60
HCLIM-METNo	0.62	0.41
HCLIM-SMHI	0.72	0.71
AROME-CNRM	0.83	0.82
MOLOCH-CNR	0.58	-0.001
COSMO-CMCC	0.62	0.63

Table 5: Same as Table 3 but for the Case 3.

Models	CASE 3 -FOEHN (WL)	CASE 3 - FOEHN (CM)
ENSEMBLE	0.91	0.90
RegCM4-ICTP	0.78	0.73
RegCM4-DHMZ	0.78	0.77
CCLM-JLU	0.92	0.89
CCLM-KIT	0.87	0.86
WRF-UHOH	0.86	0.84
WRF-FZJ-IBG3	0.78	0.81
WRF-IPSL	0.84	0.81
WRF-BCCR	0.82	0.85
WRF-UNICAN	0.86	0.82
WRF-IDL	0.84	0.84
WRF-CICERO	0.85	0.82
REMO-GERICS	0.91	0.90
HCLIM-KNMI	0.89	0.90
HCLIM-METN _o	0.90	0.83
HCLIM-SMHI	0.87	0.87
AROME-CNRM	0.89	0.91
MOLOCH-CNR	0.86	0.89
COSMO-CMCC	0.90	0.90